Foraging on host synthesized metabolites enables the bacterial symbiont *Snodgrassella alvi* to colonize the honey bee gut

Andrew Quinn[1,A], Yassine El Chazli[1,A], Stéphane Escrig[2], Jean Daraspe[3], Nicolas Neuschwander[1], Aoife McNally[1], Christel Genoud[3], Anders Meibom[2,4], Philipp Engel[1,*]

[1] Department of Fundamental Microbiology, University of Lausanne, Lausanne, Switzerland

[2]Laboratory of Biological Geochemistry, Ecole Polytechnique Fédérale de Lausanne (EPFL), Lausanne, Switzerland.

[3] Electron Microscopy Facility, University of Lausanne, Lausanne, Switzerland

[4] Center for Advanced Surface Analysis, Institute of Earth Sciences, University of Lausanne, Lausanne, Switzerland

[A] Equally contributing first authors

* Corresponding author: phillipp.engel@unil.ch

Keywords

Microbiome, microbiota, insect, symbiosis, metabolomics, NanoSIMS isotope-tracing, gnotobiotic, mass spectrometry, proteobacteria.

Summary

Nutrients from the host diet and microbial cross-feeding allow diverse bacteria to colonize the animal gut. Less is known about the role of host-derived nutrients in enabling gut bacterial colonization. We examined metabolic interactions within the evolutionary ancient symbiosis between the honey bee (*Apis mellifera*) and the core gut microbiota member *Snodgrassella alvi*. This Betaproteobacteria is incapable of metabolizing saccharides, yet colonizes the honey bee gut in the presence of only a sugar diet. Using comparative metabolomics, ^{13}C tracers, and Nanoscale secondary ion mass spectrometry (NanoSIMS), we show *in vivo* that *S. alvi* grows on host-derived organic acids, including citrate, glycerate and 3-hydroxy-3-methylglutarate which are actively secreted by the host into the gut lumen. *S. alvi* additionally modulates tryptophan metabolism in the gut, primarily by converting kynurenine to anthranilate. These results suggest that *Snodgrassella* is adapted to a specific metabolic niche in the gut that depends on host-derived nutritional resources.

Introduction

Gut bacteria and their hosts typically engage in mutualistic interactions. Metabolic exchange from the gut microbiota to the host is vital for uptake of essential nutrients, gut health and immune system function [1]. In turn, bacteria profit from a stable niche environment and frequent supply of exogenous food. Less well understood however, is the role of host secreted metabolites that benefit bacteria in the gut. Such metabolic exchange is difficult to identify due to the overwhelming contributions of the diet and microbial products towards gut metabolites.

Deciphering the extent to which host metabolite secretion drives microbial colonization of native symbionts is aided by a simple, tractable system in which diet and microbiota derived metabolites can be tightly controlled. The Western honey bee (*Apis mellifera*) provides such a system: Its gut microbiota is highly stable and composed of only 8-10 phylotypes [2,3], (i.e. clusters of bacteria sharing >97% identity in the 16S rRNA gene) many of which have longstanding evolutionary associations with their host that dates back to the emergence of social bees >80 mya [4-6]. These phylotypes are culturable and can be inoculated individually or as defined communities into gnotobiotic bees [7]. Furthermore, while the typical honey bee diet features a rich mixture of compounds found in nectar and pollen, bees can survive for extended periods on pure sugar water diets [8].

Most members of the bee gut microbiome are primary fermenters, possessing a broad range of carbohydrate degradation enzymes that enable them to utilize hemicellulose, pectin, starches, or glycosides found in pollen [3,9]. A notable exception is the Betaproteobacteria *Snodgrassella alvi*. It colonizes the cuticular surfaces of the ileum in the hindgut and displays a markedly different metabolism [10,11]. Lacking a functional glycolysis pathway, *S. alvi* profits from acids in the gut, generating energy from an aerobic TCA cycle, and biomass through gluconeogenesis. Fermentation by other microbial members has been proposed as the primary source of short chain fatty acids (SCFAs) consumed by *S. alvi*. In particular, the Gammaproteobacteria *Gilliamella* is a likely mutualistic partner for metabolic crosstalk, as the two phylotypes co-localize within biofilms attached to the cuticular surface in the ileum and share complementary metabolic capabilities [10]. Experimental evidence from *in vitro* growth

experiments bolstered this hypothesis, showing that *S. alvi* grows on the spent media of *Gilliamella*, while consuming numerous products of *Gilliamella* metabolism, such as succinate and pyruvate [12].

Although a strong case can be made for niche exploitation through bacterial cross-feeding, this hypothesis does not explain previous results in which *S. alvi* was able to mono-colonize bees fed diets of sugar water and pollen [12]. To better understand the nutrient sources that *S. alvi* exploits, we provided bees a simple (sugar water) or complex (sugar water + pollen) diet and colonized them with *S. alvi* alone, or together with strains of *Gilliamella*. Surprisingly, we found that a simple sugar water diet was sufficient for *S. alvi* to colonize the honey bee gut. Subsequent metabolomics analysis indicated that host-derived carboxylic acids enable *S. alvi* colonization. We validated this hypothesis with a series of experiments to show that (i) these compounds are synthesized by the host, (ii) *S. alvi* utilizes these compounds for growth, and (iii) the findings hold across a range of divergent *Snodgrassella* strains.

Results

S. alvi colonizes the honey bee gut in the presence of only sugar in the diet

We colonized microbiota-depleted (MD) honey bees with *S. alvi* (strain wkB2) and a mixture of *Gilliamella* strains (strains wkB1, ESL0169, ESL0182, ESL0297) alone or with both phylotypes together, and provided a diet composed of only sugar water (sucrose) or sugar water and pollen for 5 days. Colonization levels of both phylotypes were assessed by qPCR and CFU plating 5 days post inoculation (**Fig. 1A**, **Fig. S1**). *S. alvi* colonized at equivalent levels in the guts across all treatment groups, *i.e.*, sugar water in the diet was sufficient to enable *S. alvi* colonization and neither the addition of pollen to the diet nor co-colonization with *Gilliamella* significantly increased *S. alvi* loads (Wilcoxon rank sum test with *S. alvi* (sugar water) as reference group).

S. alvi depletes organic acids in the honey bee gut

We then extracted metabolites from the mid- and hindgut to search for putative *S. alvi* growth substrates originating from the host, the pollen diet, or *Gilliamella*. The presence of pollen in the gut significantly increased the abundance of nearly half of the annotated metabolites (125/233) in MD bees (**Fig. S2**). Thus, we compared results between colonized and MD bees only within each dietary treatment. When we examined mono-colonization of *S. alvi* in bees fed with sugar water, we identified multiple carboxylic acids, including citrate, 3-hydroxy-3-methylglutarate (3Hmg), and glycerate that were significantly less abundant than in the MD controls **(Fig. 1B)**. These carboxylic acids, along with others (*e.g.*, 2-ketoisocaproate, 2-ketoglutarate, and malate) were also depleted in *S. alvi* mono-colonized bees that were fed pollen **(Fig. 1B)**, despite the substantial differences in the overall metabolite profiles between the two dietary conditions. In contrast, few metabolites were significantly more abundant in *S. alvi* colonized bees relative to MD bees, with only anthranilate, a product of tryptophan metabolism, accumulating in colonized bees of both dietary treatments (**Fig. 1B**).

We then fit each metabolite with a mixed linear model to quantify how strongly metabolite changes were influenced by each of the three experimental variables across the eight experimental conditions (*i.e.*, the presence of *Gilliamella*, *S. alvi*, or pollen in the diet). This allowed us to infer which metabolites were co-produced, co-consumed, or cross-fed (and in which direction) between the two bacteria (**Fig. 1C**). For example, we found evidence supporting our initial hypothesis of metabolic cross-feeding from *Gilliamella* to *S. alvi* in the form of lactate, pyruvate and other unknown compounds that were positively affected by *Gilliamella* and negatively affected by *S. alvi* (**Fig. 1C**, **Fig. S3**). In contrast, we found no evidence of reverse cross-feeding from *S. alvi* to *Gilliamella*. Both species also compete for metabolites and act synergistically to synthesize others. Competition, or co-consumption, centered on the carboxylic acids in the bee gut, with both species depleting citrate and glycerate, and to a lesser extent, malate, and fumarate (**Fig. 1C**, **Fig. S3**). Cooperative synthesis revolved around 4 metabolites, acetate, succinate, benzoate, and an unknown. Of these, only acetate was also more abundant in mono-colonization (*Gilliamella*) than in MD controls (**Fig. 1C**, **Fig. S3**). Finally, as already observed in the

analysis of the mono-colonizations of *S. alvi*, nearly all of the metabolites were affected by pollen in a positive manner, except for citrate, glycerate, acetate, and two unknown compounds, which were unaffected, and urea, whose abundance was negatively correlated with pollen. Taken together, these results show that each of the tested variables impacts nutrient availability and metabolism of *S. alvi*.

Host ^{13}C Glucose catabolism provides *S. alvi* substrates *in vivo*

Given that pollen significantly increased the abundance of many putative substrates for *S. alvi*, we next sought to determine if these metabolites were directly supplied by the pollen or produced by the host in response to a pollen diet. First, we calculated the average abundance of these metabolites in MD bees fed sugar water versus those fed sugar water and pollen. In all cases, the average metabolite abundance was lower in bees fed only sugar water (**Fig. 2A)**. Then, we calculated the relative abundance of each metabolite extracted from the average amount of pollen consumed by each bee (26 ± 8 mg) and compared it to the amount found in pollen fed bees (**Fig. 2A**). In a simple additive model, the abundance of a metabolite in a pollen fed bee would equal the amount found in a pollen restricted bee plus the amount found in pollen. Instead, we found no clear correlation between the metabolite abundances in pollen and increased abundances in the gut of pollen fed bees. For example, negligible amounts of 3Hmg and caffeic acid were extracted from pollen relative to what was detected in the gut, while substantially more glycerate and lactate was found in pollen than in the bee gut. The wide disparity in metabolite abundances together with the fact that these metabolites are also detected in the absence of pollen in the gut suggests active metabolism by the host, i.e. nutrients in pollen are absorbed and metabolized by the bee, indirectly leading to increased abundances of host synthesized substrates for *S. alvi*.

To corroborate this hypothesis, we fed MD bees for 6 days, with 45% of the dietary sucrose replaced by 100% U-$^{13}C_6$ Glucose. Half of the bees were also provided standard pollen to assess its contribution relative to the host in the accumulation of gut metabolites. We then analyzed the resulting ^{13}C isotopic enrichments in gut metabolites with a focus on those indicated as substrates for *S. alvi*. The carboxylic

acids and non-essential amino acids were significantly ^{13}C enriched in the bee gut. In contrast, other compounds, such as kynurenine and essential amino acids did not show any enrichment **(Fig. 2B)**. The lack of isotope labelling indicates that these compounds were not actively synthesized in adult bees. Instead, they were either leftover in the gut from the larval development stage or were acquired exclusively from the diet such as in the case of essential amino acids. As expected, the average ^{13}C enrichment levels of most metabolites dropped in bees fed with pollen compared to those fed with sugar water only. The ^{13}C dilution can occur directly from non-labelled metabolites in pollen, as well as indirectly from host metabolism of pollen substrates. However, the average ^{13}C enrichment of carboxylic acids only dropped from 21 ± 6% to 17 ± 7%, which serves as further evidence that the host rather than diet is the predominant source of carboxylic acids in the gut (**Fig. 2B).** We thus concluded from this analysis that the carboxylic acids utilized by *S. alvi* are mostly *de novo* synthesized from sugar metabolism of the host.

NanoSIMS reveals transfer of host compounds to *S. alvi*

While our previous experiments suggested host nutrient foraging by *S. alvi*, the results did not provide direct evidence that *S. alvi* assimilates biomass from these compounds. Therefore, we probed the flow of metabolites from the bee to *S. alvi* using a "pulse-chase" ^{13}C isotope labelling experiment (ILE), and then measured the enrichment within *S. alvi* cells and surrounding host tissue using nanoscale secondary ion mass spectrometry (NanoSIMS) (**Fig. 3, Dataset S1**). To do so, we enriched newly emerged MD bees in ^{13}C by feeding them pure U-^{13}C glucose for four days after emergence. We then inoculated them with *S. alvi* and waited one day before switching their diet to ^{12}C-Glucose (**Fig. 3A**). This ensured that the largest *S. alvi* population increase, between 24- and 48-hours post-colonization, occurred without a dietary ^{13}C source, but still in a highly ^{13}C labelled environment **(Fig. 3B)**.

Accordingly, we measured rapid ^{13}C labelling turnover in *S. alvi* in 18 images coming from 2 bees (sampled at 48 and 72 hours post-inoculation) in which we could detect bacterial cells **(Fig. 3C, E, Dataset S2)**. The ^{13}C enrichment was substantially higher in *S. alvi* cells than in the adjacent host ileum

tissue 48 hours after inoculation, but then dropped below the levels of host tissue 72 hours after inoculation (At% = start: 5.56, end: 2.25) **(Fig. 3C)**. In contrast, the ileum tissue displayed a constant ^{13}C enrichment over the course of the experiment (At% = start: 3.31, end: 3.16), whereas the cuticle lining of the gut epithelium was comparatively less enriched initially and continued dropping to almost natural ^{13}C enrichment levels after 72 hours (At% = start: 2.58, end: 1.39) **(Fig. 3C)**.

The ^{13}C enrichment of carboxylic acids and host synthesized (non-essential) amino acids in the gut dynamically shifted in response to $^{13}C/^{12}C$ switch (**Fig. 3D, Dataset S1)**. Initially, they were highly ^{13}C enriched (38 ± 14.7%), but the labelling fell steadily to approximately half the original level (14± 5.8%) within 48 hours (**Fig. 3D)**. As a control, we found that essential amino acids (non-host synthesized) were only enriched to the level of natural ^{13}C abundance (1.11%) throughout the experiment. Thus, these results show that products of host glucose metabolism are actively used by *S. alvi* to build its biomass during early colonization.

In vitro growth assays confirm active metabolism by *S. alvi*

We next tested whether the putative host synthesized substrates were sufficient for growth of *S. alvi* as sole carbon sources in a chemically defined liquid medium "Bee9", which we derived from standard M9 media (**Fig. 4A**, **Dataset S3**). We utilized Bee9, after finding that *S. alvi* consumes amino acids present in standard M9 previously used to grow this bacterium [12]. Only three metabolites (citrate, isocitrate, and malate) supported growth as sole carbon sources in this condition. However, the addition of 3Hmg, fumarate, succinate, gamma-aminobutyrate (Gaba), kynurenine, or urea to Bee9 + citrate significantly improved the maximal growth rate of *S. alvi* versus with citrate alone (**Fig. 4B**). In particular, 3Hmg and Gaba had dramatic effects on growth rates, increasing them respectively 3.52 ± 0.10 and 2.76 ± 0.04 fold.

Analysis of the spent media revealed that all tested metabolites, except for the glucose negative control, were depleted by *S. alvi* (**Fig. S4**). This further confirmed that the identified host-derived organic acids are growth substrates of *S. alvi*. Unlike the results from our colonization experiments, *S. alvi* produced

numerous carboxylic acids, which varied based on the carbon source. For example, acetate was a metabolic substrate, but it was also produced in the presence of pyruvate or 3Hmg. Meanwhile, alpha-ketoglutarate, 2-oxoisovalerate, malate and succinate were produced across most growth conditions (**Fig 4C**). Consistent with the *in vivo* metabolomics, we detected production of anthranilate when kynurenine was added to the media. Additionally, we also detected the production of kynurenic acid and tryptophan (**Fig. 4D).** *S. alvi* wkB2 encodes a putative kynureninase gene in its genome (SALWKB2_0716) that is likely responsible for the conversion of kynurenine into anthranilate. Interestingly, this gene seems to have been acquired by horizontal gene transfer as indicated by a phylogenetic analysis **(Fig. S5)**: apart from other *Snodgrassella* strains, the closest sequences of the kynureninase gene were not found in other Neisseriaceae, but in more distantly related Betaproteobacteria (genera *Pusilimonas* and *Alcaligenes*) and in Gammaproteobacteria (genera *Ignatzschineria* and *Acinetobacter*).

Colonization without an exogenous nutrient source is conserved across strains of the genus *Snodgrassella*

As a final step, we examined whether our results were unique to *S. alvi* wkB2 or were more generally applicable to the genus by inoculating bees with five divergent strains of *Snodgrassella*, three native to honey bees and two native to bumble bees. We also lengthened the colonization experiment from five to ten days to account for a potential delay in colonization of the honey bee gut by non-native strains. All five strains successfully colonized bees fed only sugar water. However, the efficiency and extent of colonization varied between strains. Strains of *S. alvi* native to honey bees colonized consistently, while non-native strains sometimes failed to colonize (Aggregate Colonization Success: 100% vs. 70%; Fisher's Exact test: $p < 0.001$) (**Fig. 5A**). The gut metabolomic comparison between successfully colonized versus MD honey bees was qualitatively similar to our initial results. Carboxylic acids, such as 3Hmg, malate, fumarate, succinate, isocitrate, and glycerate were significantly less abundant in colonized guts vs MD controls across three or more of the *S. alvi* strains tested. The levels of purine

and amino acid precursors hypoxanthine and urea were also depleted in the guts of colonized bees, while anthranilate again accumulated in all colonized bees (**Fig. 5B, Fig. S6**). These results show that the utilization of host-derived carboxylic acids is a conserved phenomenon in the genus *Snodgrassella* and facilitates gut colonization independent of bacterial cross-feeding or diet-derived nutrients.

Discussion

There is an increased focus on the role of host-derived metabolites in feeding extracellular symbionts across animal models. Multiple independent studies have demonstrated how these bacteria exploit their host, grazing on the mucosal lining in the murine gut or being chemoattracted by the chitin synthesized in the light organ of squid [13-20]. Pathogenic *Salmonella* was found to exploit host-derived aspartate, malate and lactate to invade the mammalian gut [21-23]. Recently, commensal gut species were found to utilize host synthesized lactate, 3-hydroxybutyrate and urea in mice [24]. Our study demonstrates that such host-derived metabolites can represent the major carbon source for certain gut bacteria facilitating colonization and growth, independent of the diet or cross-feeding.

We took advantage of the bee as a model host to drastically minimize confounding factors, colonizing bees with a single bacterium, *S. alvi*, while restricting the host to a sole dietary substrate that is undigestible for this bacterium. We then utilized ^{13}C-glucose labelling to show that organic acids measured in the gut are synthesized by the host from dietary sugars which are then assimilated by *S. alvi* cells during gut colonization. The ^{13}C enrichment of *S. alvi* was initially higher than in the surrounding host tissue, but then dropped after the host diet was switched to ^{12}C-glucose. These dynamics are consistent with the hypothesis that *S. alvi* utilizes host metabolites that are derived from simple carbohydrates catabolism in the bee diet, rather than from grazing on host epithelium lining the gut (**Figure 6**). Finally, we demonstrated that these organic acids sustain growth of *S. alvi in vitro*.

Our results provide new context to the substantial body of research on bacterial colonization of the bee gut. The consistent depletion of host-derived acids linked to the TCA cycle complements findings that

these metabolites are depleted in bees colonized with individual microbes including *S. alvi*, *Gilliamella*, *Lactobacillus* Firm-5 and *Bartonella apis*, as well as when colonized with a full microbial community [12,25,26]. Thus, foraging on host-derived compounds, although not always essential, may be widespread in the native bee gut community. Yet, in the specific case of *S. alvi*, these host-derived nutrients seem to be key for colonization. This is supported by a previous study which found that all genes of the TCA cycle and multiple genes associated with organic acid and ketone body degradation, provide a strong fitness advantage to *S. alvi* to grow in the bee gut [27].

Strikingly, two major metabolic functions conserved across all five strains of *S. alvi* (3Hmg consumption and anthranilate production), were associated with unique features in the metabolic pathways of *S. alvi*, providing evidence for adaptation to a specialized host niche. *S. alvi* possesses a non-canonical TCA cycle (**Figure 6**); lacking a glyoxylate shunt it is unable to grow on acetate alone, but the substitution of acetate:succinate CoA-transferase for the canonical succinyl-CoA synthetase means that acetate, rather than acetyl-CoA, is a key driver of the TCA cycle [28]. Interestingly, we found that 3Hmg consumption results in the production of acetate when *S. alvi* is grown on 3Hmg *in vitro*. Therefore, we postulate that host-derived 3Hmg enhances growth of *S. alvi* via the production of acetate which increases the flux through the TCA cycle (**Figure 6**). 3Hmg is an intermediate of the host's isoprenoid biosynthesis, leucine degradation and ketone body metabolism, though why this metabolite is released into the gut remains elusive.

The second unique metabolic feature of *S. alvi*, the production of anthranilate, likely depends on the enzymatic activity of a kynureninase gene identified in the genome of *S. alvi* converting host- and/or diet-derived kynurenine into anthranilate as confirmed by our *in vitro* growth experiments (**Figure 6**). Intriguingly, this gene is the only enzyme annotated in the tryptophan degradation pathway of *S. alvi*; it is highly conserved in the entire genus and has likely been acquired by horizontal gene transfer, suggesting that it carries a conserved function that is specific to the symbiosis between *Snodgrassella* and its bee hosts.

The release of relatively valuable metabolites into the gut could be a way for the host to control community assembly and facilitate the colonization of particularly beneficial gut symbionts [29]. While

the full gut microbiota has been shown to carry out several important functions for the host, the specific role of *S. alvi* has remained elusive. This bacterium colonizes the epithelium of the ileum and thus may have a protective role against pathogen invasion [30]. However, it is also possible that its metabolic activities, such as the conversion of kynurenine into anthranilate, may have a positive effect on the host. Kynurenine is important during the larval stage of bee development, but it is also associated with neuronal defects (*e.g.*, hyperactivity and motor disfunction) in insects and vertebrates [31-33]. In contrast, anthranilate is an important precursor of the essential amino acid tryptophan and several neurotransmitters such as serotonin, tryptamine and various indole derivatives, all of which are highly beneficial to bees [34]. In fact, indoles synthesized from tryptophan by *Lactobacillus* Firm-5 species in the gut were recently linked to enhanced memory and learning in honey bees [35]. Finally, we also note that the metabolism of urea by *S. alvi* could have a beneficial effect on the host. Urea constitutes a major waste product in mammals and insects. In turtle ants, ancient, specialized gut bacteria are able to recycle large amounts of nitrogen from urea into both essential and non-essential amino acids [36]. We found that urea is more abundant in the bee gut when exogenous nitrogen was absent from the diet, indicative of higher metabolic turnover and waste, which *S. alvi* could alleviate through urea fixation.

Our results and analysis fit within the context of limitations that we enumerate below. We examined a portion of the total gut metabolome that is amenable to analysis with gas chromatography. Further compounds of interest may be detected using complimentary analytical capabilities. While we have shown that host-derived compounds can sustain growth of *S. alvi*, the tested conditions did not reflect the natural state of the bee gut with a full microbial community and a metabolically rich diet that alters between bee bread, pollen, honey and flower nectar. Therefore, we cannot exclude that dietary or microbially derived metabolites contribute to the growth of *S. alvi* in the native gut. In fact, we found *in vivo* evidence for cross-feeding of lactate and pyruvate from *Gilliamella*, as well as for pollen as an indirect source of key organic acids in the gut. However, these nutrient sources seem to play a minor role relative to the host, as the colonization levels of *S. alvi* did not differ significantly when pollen and/or *Gilliamella* were present. This is consistent with a previous study, which showed that the total abundance of *S. alvi*, in contrast to most other community members, does not change between nurse

and forager bees that have different dietary preferences, nor does it change when pollen is removed from the diet of fully colonized bees under laboratory conditions [37].

How host synthesized organic acids reach the gut lumen remains elusive (**Figure 6**). While leakage from host cells across the epithelial barrier is possible, transport via the malpighian tubules upstream of the ileum seems more likely, as they excrete nitrogenous waste and other metabolites into the gut while also regulating osmotic pressure in the hemolymph [38,39]. Future work may resolve this question through careful dissection and metabolomic analysis of the malpighian tubules and the ileum, possibly with the assistance of labeled compounds injected into the bee thorax.

Methods

Bacterial culturing

Table S1 lists all strains used in this study. Strains were isolated by directly plating gut homogenates on brain heart infusion agar, or by first culturing them in Insectagro™ (Gibco) liquid media under microaerophilic conditions for 48 hours before colonies were streaked on plates. Species identity was confirmed by 16S rRNA gene sequencing. Strains were grown on liquid Insectagro™ media for 18 hours and then diluted in Phosphate buffer saline (PBS) and 25% glycerol at OD_{600} =1. Solutions were kept frozen at -80 °C until just before colonization, when they were thawed on ice, diluted 10-fold with PBS and mixed 1:1 with sterile sugar water (1kg/L of sucrose in water).

Experimental colonization of gnotobiotic bees

All honey bees were collected from hives at the apiary of the University of Lausanne. A different hive was selected for each colonization replicate. Microbiota-free bees were raised according to established protocols [40]. Briefly, frames containing capped brood were taken from the hive and washed quickly with a towel soaked in 3% bleach. Pupae of the appropriate age were then removed from the frames and placed into sterile emergence boxes containing sterile sugar water. The boxes were placed in an incubator at 35 °C for two days. Emerged bees were then randomly transferred to separate, sterile cages assembled from plastic drinking cups and Petri dishes. Concurrently, 2 bees from each emergence box were sacrificed and their homogenized guts plated on agar plates to check for sterility.

Bees were colonized one by one with 5 µl of bacterial solution, or corresponding blank control, after starving them of sugar water for 1-2 hours, stunning them on ice for 5 minutes, and transferring them with tweezers to individual microcentrifuge tubes that were cut to enable insertion of a pipette tip. Sugar water and pollen (when specified) were provided to cages *ad libitum* throughout each experiment. Mono and co-colonizations of bees with *S. alvi* wkB2 and the four *Gilliamella* strains were performed five times, using different hives for each treatment. Not all conditions were run in each experiment due to technical difficulties preparing the treatment groups and the GC-MS analysis was only carried out for

a subset of the samples (see **Table S2** for details**)**. The colonization experiment with the divergent *Snodgrassella* strains isolated from honey bees and bumble bees was carried out twice (see **Table S3** for details).

Five days after colonization, bees were anesthetized with CO_2, placed on ice, and dissected with sterile forceps. Whole guts, minus the crop, were homogenized in a bead beater (FastPrep-24, MP) in tubes containing PBS and glass beads. The samples were each immediately divided into three aliquots. One was plated to count Colony Forming Units (CFUs). Another aliquot of 500 µl was centrifuged for 15 minutes at 4 °C and 20,000 g^{-1} and the liquid supernatant snap frozen in liquid nitrogen and stored at -80 °C until metabolomic extraction. The third aliquot was frozen directly until DNA extraction.

Isotope tracing experiments

To assess the ^{13}C metabolite enrichment in the bee gut, microbiota-depleted emerged bees were provided a 45:65 ratio of 99% U-^{13}C glucose (Cambridge Isotope Laboratory) and naturally abundant (N/A) sucrose (Sigma Aldrich) in water for 5 days in the first experiment. Bees were then sacrificed, and the guts extracted as previously described.

For the NanoSIMS time-course colonization experiment, newly emerged microbiota-depleted bees were divided into two cages and provided pure 99% U-^{13}C glucose (treatment) or ^{12}C glucose (control) in water for 5 days (pulse) before switching both cages to a ^{12}C glucose diet (chase). On the morning of the 4th day all bees were starved for 1.5 hours and colonized with *S. alvi* wkB2. The ^{13}C glucose solution was replaced with a ^{12}C glucose solution 24 hours later. Bees were harvested at 0, 8, 24, 32, 48, 56, 72 hours after inoculation. This overlap of colonization and ^{13}C glucose feeding was done to maximize the number of bacterial cells in the TEM sections and to reduce the dilution of ^{13}C label due to metabolic turnover. For each timepoint and both cages (^{13}C and ^{12}C glucose treatment), the ileum of 4 bees were dissected. One gut was immediately preserved for electron microscopy and NanoSIMS, while the other three guts were homogenized and aliquoted for CFU plating and metabolite extraction **(Fig. 3)**. The control samples (from the cage provided with ^{12}C glucose) were used to determine the natural ^{13}C

abundance in the bee tissue and *S. alvi* cells. Image metadata and Raw NanoSIMS region of interest (ROI) values can be found in **(Data availability)**.

Quantification of bacterial loads

Bacterial loads of viable *S. alvi and Gilliamella* cells in the gut were quantified based on CFUs by plating serial dilutions of gut homogenates of individual bees on brain heart infusion agar (BHIA) followed by 48h of incubation at 35 °C in an 5% CO_2 incubator. DNA extraction was carried out by adding 250 uL of 2x CTAB to frozen gut homogenates. The mixture was homogenized at 6 m/second for 45 seconds in a Fast-Prep24TM5G homogenizer (MP Biomedicals) and centrifuged for 2 minutes at 2000 rpm. DNA was extracted in two-steps with Roti-Phenol and Phenol:Chloroform:Isoamylalcohol (25:24:1), then eluted in 200 ul DNAse/RNAse water and frozen. qPCR was run using target specific primers for Apis mellifera actin, and specific 16S primers for *S. alvi* and *Gilliamella spp.* used in [12].

Metabolite extractions

Frozen gut samples were divided and extracted via two established methods for short chain fatty acids (SCFAs) and soluble metabolites. SCFAs were extracted with 750 uL diethyl ether from 75 uL of gut supernatant that was first acidified with 5 uL of 11% HCl. 200 uM isovalerate (Sigma Aldrich) was used as an internal standard. The solvents and resulting two-phase mixture were kept cold at -20 °C and vortexed 3x for 30 seconds. The samples were then centrifuged for 3 minutes at 4 °C and 13000 g^{-1}, and 80 uL of the ether phase was removed to a glass GC vial (Agilent). The sample was derivatized with 20 ul MTBSTFA + 1% TBDMS (Sigma Aldrich) for 1 hour at 30 °C [41].

Soluble metabolites were extracted via a modified Bligh and Dyer protocol [42]. A (5:2:1) mixture of methanol (Sigma Aldrich) and chloroform (Sigma Aldrich) and double distilled water was chilled to -20 °C and 800 uL added to 100 ul of gut homogenate. A mixture of norleucine (Sigma Aldrich), norvaline (Sigma Aldrich), and ^{13}C glucose (Cambridge Isotopes) was used as internal standards. The samples were vortexed three times for 30 seconds and extracted at -20 °C for 90 minutes. The samples

were then centrifuged at 13,300 g^{-1} and 4 °C for 5 minutes. Liquid supernatant was transferred to a new tube and 400 uL of cold chloroform:methanol (1:1) was added to the insoluble material. The samples were again vortexed three times, extracted for 30 minutes at -20 °C, centrifuged, and the two supernatants were combined. Phase separation was achieved by adding 200 uL of water and centrifuging at the same conditions. The upper phase was then dried overnight in a speed vacuum. The sample was derivatized with 50 ul of 20mg/ml methoxyamine hydrochloride in pyridine (Sigma Aldrich), for 90 minutes at 33 °C followed by silylation with 50 ul of MSTFA (Sigma Aldrich) for 120 minutes at 45 °C.

GC-MS analysis

Samples were analyzed on an Agilent 8890/5977B series GC-MSD equipped with an autosampler that injected 1 uL of sample onto a VF-5MS (30m x 0.25 mm x 0.25 um) column. The SCFA samples were injected with a split ratio of 25:1, helium flow rate of 1 ml/min, and inlet temperature of 230 °C. The Oven was held for 2 minutes at 50 °C, raised at 25 °C/min to 175 °C and then raised at 30 °C/minute to 280 °C and held for 3.5 minutes. The MSD was run in SIM mode with 3 target ions for each compound. The Soluble metabolite samples were injected with a split ratio of 15:1, helium flow rate of 1 ml/min and inlet temperature of 280 °C. The Oven was held for 2 minutes at 125 °C, raised at 3 °C/minute to 150 °C, 5 °C/minute to 225 °C, and 15 °C/minute to 300 °C and held for 1.3 minutes. The MSD was run in scan mode from 50-500 Da at a frequency of 3.2 scan/second.

Metabolomics data analysis

Mass spectrometry features were identified by spectral matching to the NIST17 mass spectra library or to in house analytical standards. Features were then extracted using the MassHunter Quantitative Analysis software (Agilent). Data normalization and analysis was performed using custom R scripts (See Data availability). The effect of diet, and colonization with *S. alvi* and *Gilliamella* were assessed by fitting z-score normalized metabolite abundances to a mixed linear model using the lmm2met

package in R with diet, *S. alvi* and *Gilliamella* as fixed effect factors and experimental replicate as a random effect [43]. The significance of each fixed effect was then adjusted by the Benjamini, Hochberg, and Yekutieli method to control for false discovery. Mass isotopologues were adjusted to account for natural isotope abundances following published procedures [44,45].

TEM section preparation and NanoSIMS analysis

Bee guts were dissected, the ileum was cut away from the rest of the gut and fixed in glutaraldehyde solution (EMS, Hatfield, PA, US) 2.5% in Phosphate Buffer (PB 0.1M pH7.4) (Sigma, St Louis, MO, US) for 2 hours at room temperature (RT) and kept at 4°C until sample preparation. Ileum pieces were rinsed 3 times for 5 minutes in PB buffer and then postfixed with a fresh mixture of osmium tetroxide 1% (EMS, Hatfield, PA, US) with 1.5% potassium ferrocyanide (Sigma, St Louis, MO, US) in PB buffer for 2 hours at RT. The samples were then washed three times in distilled water and dehydrated in acetone solution (Sigma, St Louis, MO, US) at graded concentrations (30%-40min; 70%-40min; 100%-1h; 100%-2h). Dehydration was followed by infiltration in Epon resin (Sigma, St Louis, MO, US) at graded concentrations (Epon 1/3 acetone-2 hours; Epon 3/1 acetone-2 hours, Epon 1/1-4 hours; Epon 1/1-12 hours) and finally polymerized for 48 hours at 60°C in an oven. Thin sections of 100 nanometers (nm) were cut on a Leica Ultracut (Leica Mikrosysteme GmbH, Vienna, Austria) and picked up on copper slot grid 2x1mm (EMS, Hatfield, PA, US) coated with a Polyetherimide (PEI) film (Sigma, St Louis, MO, US). Sections were poststained with uranyl acetate (Sigma, St Louis, MO, US) 2% in H_2O for 10 minutes, rinsed several times with H_2O followed by Reynolds lead citrate for 10 minutes and rinsed several times with H_2O.

Large montages with a pixel size of 6.9 nm covering areas of around 120x120 µm were taken with a transmission electron microscope Philips CM100 (Thermo Fisher Scientific, Hillsboro, USA) at an acceleration voltage of 80kV with a TVIPS TemCam-F416 digital camera (TVIPS GmbH, Gauting, Germany) and the alignment was performed using Blendmont command-line program from the IMOD software [46].

Four holes were made using the electron beam at the four corners of the montage to localize the area of interest for NanoSIMS imaging. Then the slot grid was deposited on 1 µL of distilled water on a 10 mm round coverslip and left to dry for 10 minutes. The slot grid was detached, letting the section attach to the coverslip.

After being coated with a 15nm gold layer to evacuate a potential build-up of a charge during the NanoSIMS analyses, the samples were analyzed by a NanoSIMS 50L (CAMECA). A primary beam of 16 keV Cs+ ions was focused to a spot size of about 100 nm on the sample surface, causing the sputtering of atoms and small molecules from the first 5-10 nm of the sample. Negative secondary ions were directed and focalized into a single beam before reaching the magnetic sector of the mass spectrometer where the ions were separated. The species of interest ($^{12}C^{14}N$- and $^{13}C^{14}N$- for this study) were then measured simultaneously using Electron Multipliers. To resolve the interference between $^{13}C^{14}N$- and $^{12}C^{15}N$-, two slits (ES and AS) were used to achieve a mass resolution higher than 10000 (Cameca definition), [47].

In the imaging mode, selected areas of 25x25 µm were implanted using a strong beam (using diaphragm D1-1 (diameter 750 µm) and a current of 16 pA) to remove the gold coating and reach stable emission conditions. After optimization of the extraction of the secondary ions, the area was imaged by scanning a smaller beam (~100 nm, using diaphragm D1-5 (diameter 100 µm) and a current of 0.45 pA) with a 256x256 pixel resolution and a dwell time of 5µs/pixel. For each image, 10 layers were acquired. The image processing was performed using "L'image" software (Larry Nittler, Carnegie Institution of Washington). The 10 layers were aligned and stacked, 44 ms deadtime correction was applied. Regions of interests (ROI) were manually drawn around bacterial cells, gut epithelium layer, and bulk host cells. Data was extracted and reported in table **(Dataset S1)**. At% enrichment was calculated in R using the data.table package. At% enrichment formula: $13C\ At\% = {}^{14\mathrm{N}\ 13\mathrm{C}}/_{(14\mathrm{N}\ 13\mathrm{C}\ +\ 14\mathrm{N}\ 12\mathrm{C})} \times 100.$ **(Fig. S7).**

In vitro growth of *S. alvi*

S. alvi was cultured in Bee9 media, an M9 derived, minimal defined media containing essential vitamins and mixtures of organic acids (see recipe in **Dataset S3**). Growth assays were performed in 96-well plates (Corning costar) at 35 °C, 5% CO_2, with continuous orbital shaking (H1 Synergy, Biotek). OD_{600} measurements were taken every 30 min for 20 hours. All conditions were independently replicated three times. For metabolomics measurements, plates were immediately placed on ice at the end of each experiment, and liquid was transferred to microcentrifuge tubes. The tubes were then centrifuged at 13,30 g^{-1} and 4 °C for 30 seconds, and the liquid supernatant was then snap frozen in liquid nitrogen and stored at -80 °C for metabolomic analysis.

Phylogenetic analysis of the kynureninase gene family

The kynureninase protein sequence of *S. alvi* wkB2 was retrieved from NCBI (WP 025330329.1), and blasted (NCBI, BlastP) against the "nr" database. Based on the BlastP hits, 227 divergent amino acid sequences were exported in fasta format and aligned using MUSCLE [48] with standard parameters. Tree inference and bootstrap validation were performed using IQtree with the following command: "iqtree-omp -s kyn_sequences_muscle.aln -nt 6 -m TEST -bb 1000" [49]. The tree topology was visualized using the ITOL online viewer (https://itol.embl.de/).

Figures

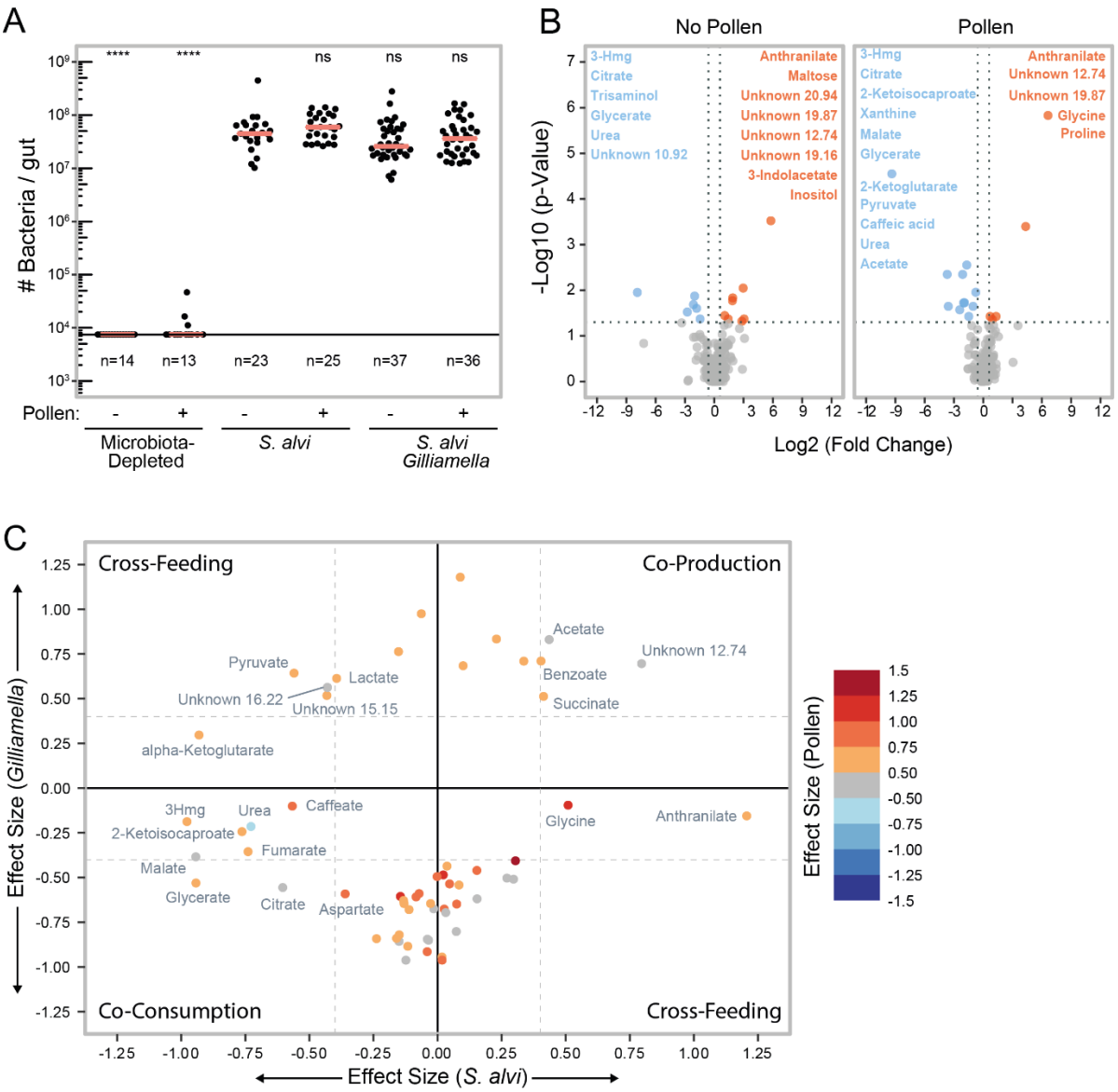

Figure 1. *S. alvi* colonizes bees fed with sugar water only and depletes host, pollen, and *Gilliamella* derived metabolites. (A) Number of *S. alvi* cells (number of bacterial genome equivalents) per bee gut determined by qPCR using *S. alvi*-specific 16S rRNA gene primers. Each value represents the number of cells in a single bee gut, red bars represent the median, horizontal black line represents qPCR limit of detection (LOD = < 7.5e+03). For each treatment, the presence/absence of pollen in the diet is indicated by +/- sign. Significance determined by Wilcoxon rank sum test with *S. alvi* (pollen -) as reference group, ns, non-significant; ****$P < 0.001$. **(B)** Significantly differentially abundant gut metabolites between *S. alvi* colonized and microbiota-depleted (MD) bees. Significantly depleted and

produced metabolites are shown in blue and orange, respectively. Adjusted significance values were calculated using Wilcoxon rank sum test, and Benjamini-Hochberg correction, using the MD samples as a reference. **(C)** Results from mixed-linear modelling show the contributions (fixed effect sizes) of microbial colonization and diet towards z-score normalized metabolite abundances. Only metabolites significantly correlated with *S. alvi* colonization are named. Large values (+/-) indicate a strong correlation between a factor and a corresponding change in metabolite abundance. Values centered around zero (inside the dotted lines) are not significant. The effect size of pollen is indicated by the color of each metabolite, red colors indicate significantly positive correlation, while blue is a significant negative correlation. The four corners of the graph represent the four types of metabolic interactions between *S. alvi* and *Gilliamella* (from the top left: cross-feeding from *S. alvi* to *Gilliamella*, co-production by both bacteria, cross-feeding from Gilliamella to *S. alvi*, co-consumption). Carboxylic acids are grouped principally on the lower-left section of the plot indicating they are less abundant with *S. alvi* and *Gilliamella* colonization.

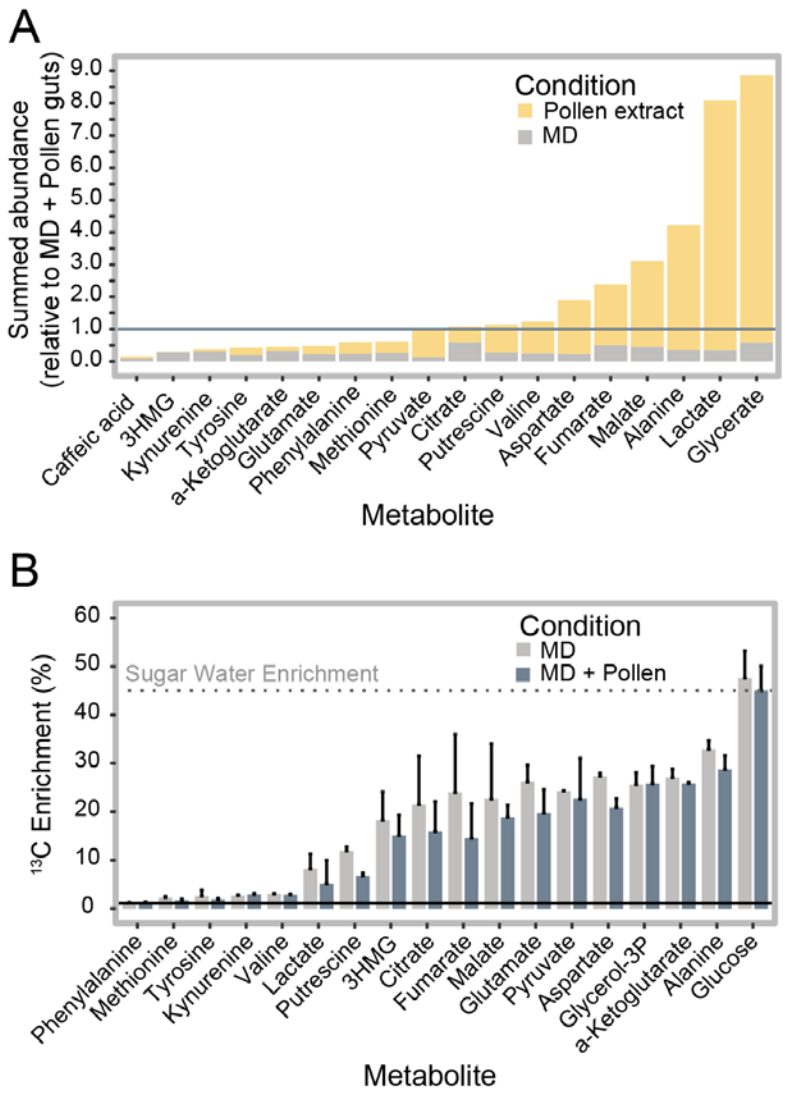

Figure 2. Pollen extract composition and isotope labelling reveals host origin of *S. alvi* substrates. **(A)** Metabolite abundances in pollen extract (PE, yellow) do not correlate with increased abundances in the guts of pollen fed bees. The summed average abundances of metabolites in sugar water fed bees and in PE are shown relative to the abundance of the same metabolite in pollen fed bees. Summed values across metabolites ≈1.0 would indicate pollen was a direct dietary source of most metabolites. Quantitates from pollen extract were adjusted based on average total pollen consumption per bee. **(B)** The average (n=4) ^{13}C metabolite enrichment (%) in bee guts shows that carboxylic acids and non-essential amino acids become highly labelled upon feeding ^{13}C-glucose to MD bees. Dark and light bars indicate, respectively, absence and presence of pollen in the diet. The solid line denotes the natural ^{13}C enrichment (1.108%), while the dashed line denotes ^{13}C enrichment of sugar water solution fed to experimental bees.

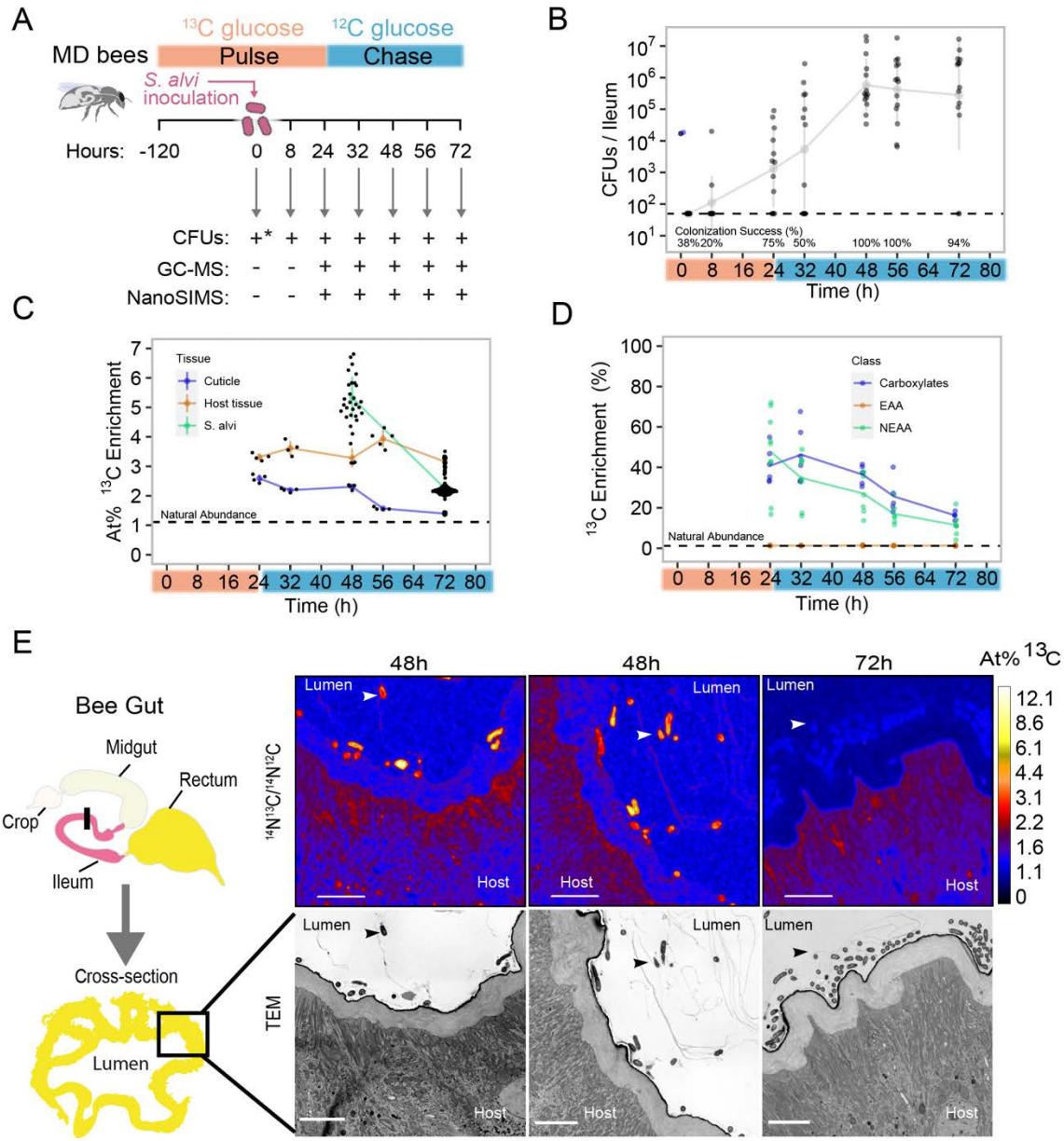

Figure 3. *S. alvi* builds biomass from substrates derived from the glucose metabolism of the host. **(A)** Experimental design of the pulse-chase isotope labelling gnotobiotic bee experiment. Newly emerged MD bees were fed 100% ^{13}C glucose for 4 days, colonized with a defined quantity of *S. alvi* and then the ^{13}C glucose was replaced by ^{12}C glucose 24 hours after colonization. The timeline indicates when bees were sampled for CFU plating, GC-MS and NanoSIMS analysis. **(B)** Colonization levels of *S. alvi* in the ileum until 72 hours post inoculation show the initial strong colonization bottleneck and subsequent exponential increase in cell numbers. Colonization success is indicated as percentage of bees with detectable CFUs. Blue dots indicate the inoculum of *S. alvi* (OD= 0.1). **(C)** The average At%

^{13}C enrichments of *S. alvi* cells decreases rapidly, while the enrichment of host cells and epithelium remains constant over 72 hours in ileum cross-sections imaged with NanoSIMS. Each data point represents the mean of regions of interest (ROI); bacterial ROIs consist of single bacterial cells, while epithelium and host cells ROIs represent the total area encompassing epithelium or host cell tissue in each image. ROI raw counts and calculated enrichments are listed in **Dataset S1**. **(D)** ^{13}C enrichment of metabolites in the gut steadily decreases in the ^{12}C chase phase. Values represent the average ^{13}C enrichment of a given metabolite across the bees sampled at that timepoint. Average values and colors are shown by metabolite class: carboxylic acids (violet), non-essential amino acids (green), essential amino acids (brown). Measured metabolites are listed in **Dataset S1**. The dotted line at 1.1 % indicates the natural ^{13}C abundance calculated from NanoSIMS images of ^{12}C control bees. **(E)** NanoSIMS and corresponding TEM images of 2 different ^{13}C labeled bees at 48 and 72 hours after inoculation. White arrows indicate *S. alvi* cells. At% ^{13}C represents percentage of ^{13}C atoms; the natural ^{13}C abundance is ~1.1 at%. Scale bars = 5 uM.

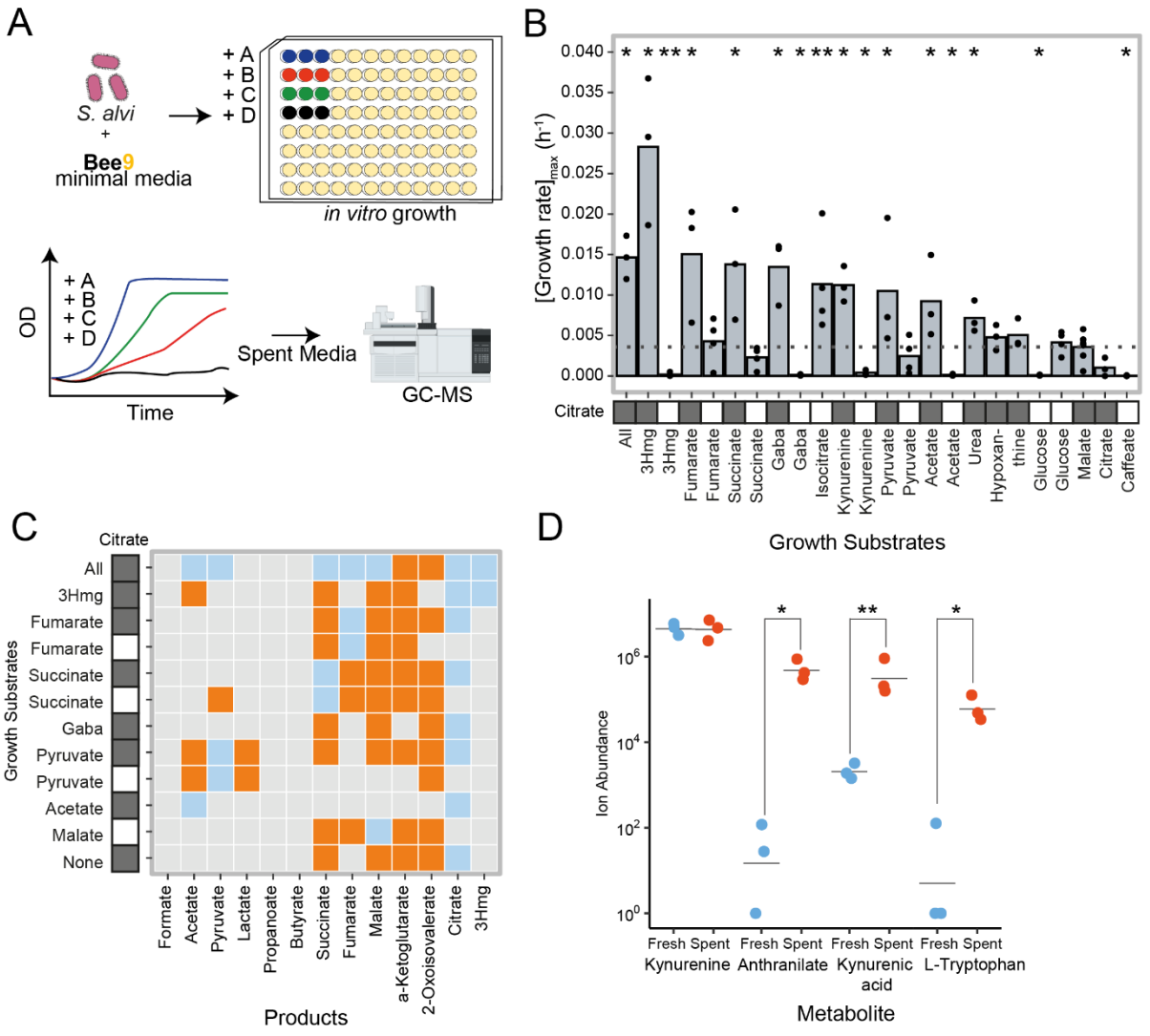

Figure 4. **Host synthesized compounds enhance *S. alvi* growth *in vitro*. (A)** Schematic diagram depicting growth and spent supernatant analysis. The "Bee9" media was derived from M9 base media (**Dataset S3**). **(B)** The maximum growth rate across single carbon sources with (grey boxes) or without (white boxes) citrate added to the medium, reveals that growth on citrate + 3Hmg was faster than for all other conditions, including "All", where all substrates were pooled together. The average value (bars) was calculated from the individual biological replicates (dots). Significant differences between growth rates were calculated using a Wilcoxon rank sum test, with growth on citrate as the reference state (dotted line). **(C)** Production (orange squares) of carboxylic acids in the spent supernatant varies with growth substrates (light blue squares). Acetate is a growth substrate, but also is produced with either pyruvate or 3Hmg in the media. **(D)** Addition of kynurenine to the media leads to the production of

anthranilate, kynurenic acid, and L-tryptophan. Significant changes between fresh and spent media were calculated using a paired t-test. (* $P < 0.05$, ** < 0.01, *** < 0.001, **** < 0.0001).

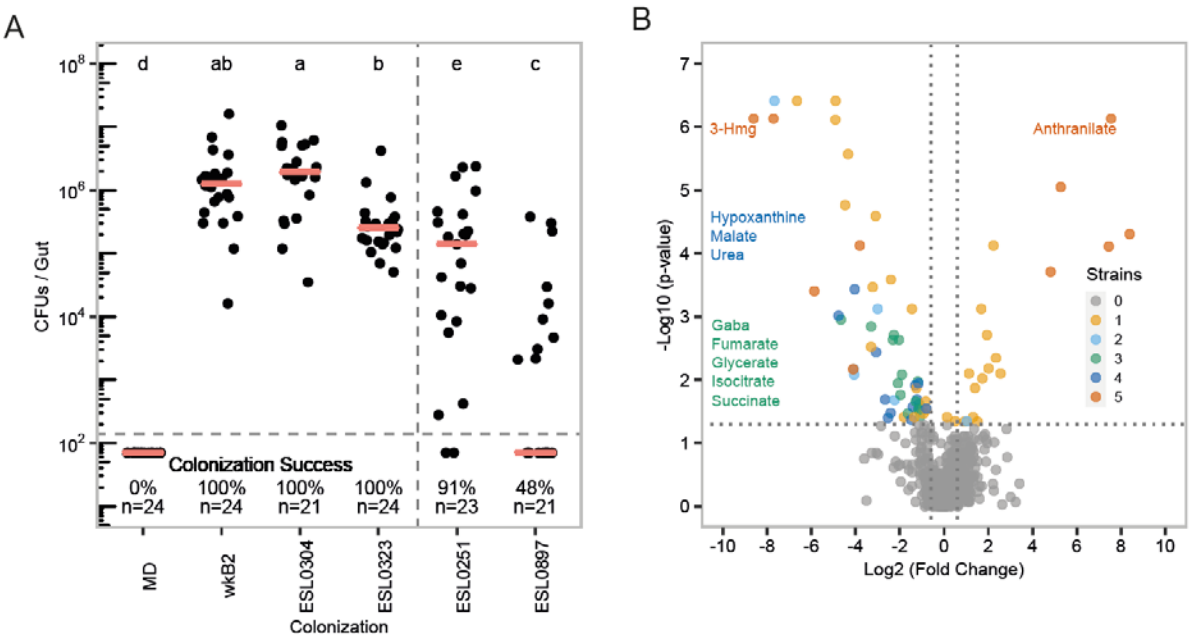

Figure 5. Divergent *S. alvi* strains colonize the honey bee gut in the presence of only sugar in the diet and deplete a similar set of metabolites. (A) Colonization levels of divergent *S. alvi* strains in monocolonized bees. Each value represents the bacterial load in one bee gut, colonization success is indicated as percentage of bees with detectable CFUs. Pink bars denote the median of CFUs/gut for each group. The limit of detection is shown with a horizontal dash line. The vertical dotted line divides *S. alvi* strains native to *A. mellifera* and *Bombus sp.* Groups not connected by the same letter are significantly different as based on an ANOVA followed by Tukey's HSD test. (**B**) Volcano plot of gut metabolites showing the similarities in metabolite changes from colonized vs MD bees across strains. Each metabolite is plotted 5 times (once per *S. alvi* strain), and color coded by the number of strains in which it is significantly differentially abundant vs the microbiota-depleted (MD) bees control. Only 3Hmg and anthranilate were significantly depleted or enriched by all five strains, while four of the strains depleted hypoxanthine, malate, and urea, and three of the five depleted Gaba, fumarate, glycerate, isocitrate and succinate.

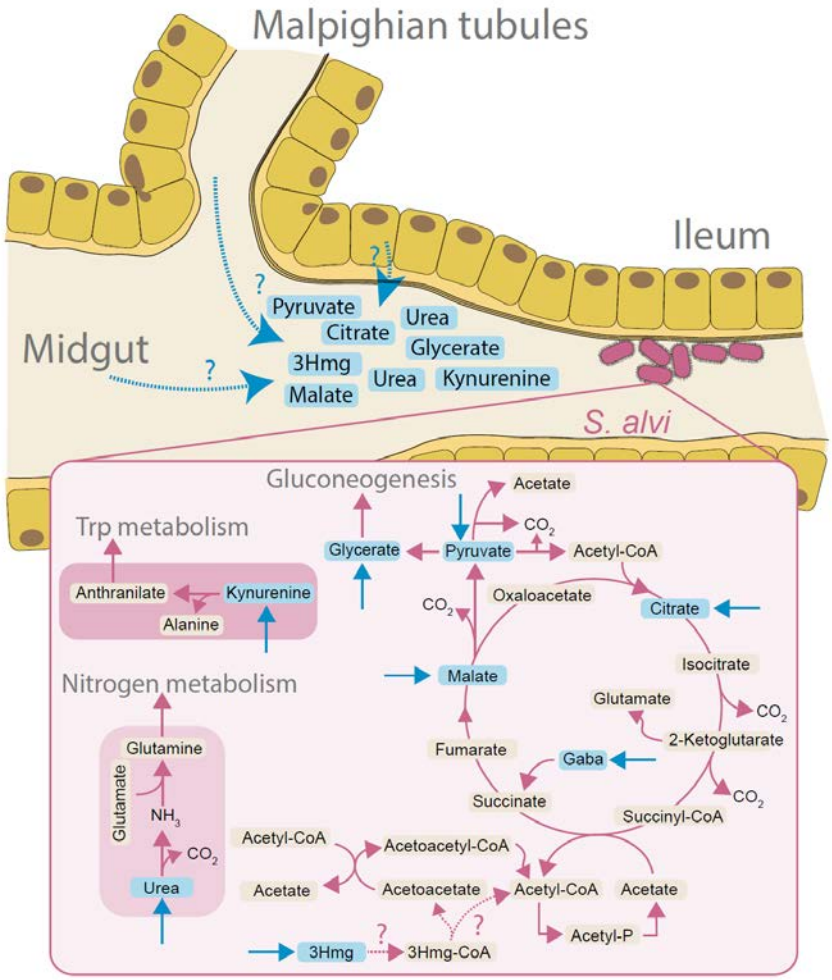

Figure 6. Schematic depicting *S. alvi* metabolism of host derived compounds in the ileum. Host metabolites (blue) enter the ileum through the epithelial cells, or through the malpighian tubules upstream of the ileum. *S. alvi* primarily utilizes the TCA cycle to generate energy, then synthesizing biomass through gluconeogenic reactions. 3Hmg provides a source of acetate to fuel the TCA cycle. However, the reactions synthesizing the first two steps (dotted pink arrows) have not been annotated in the genome. Additionally, host synthesized urea is a source of nitrogen, and kynurenine is converted to anthranilate as part of tryptophan metabolism. Blue arrows indicate substrates provided by the host metabolism.

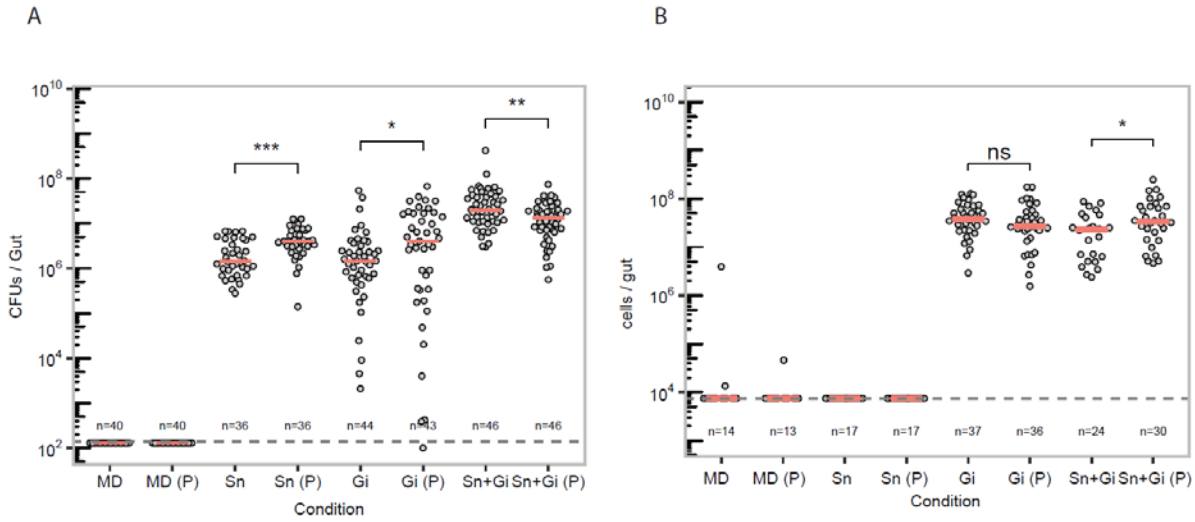

Figure S1. Total number of bacterial colonization and colonization levels of *Gilliamella* per bee gut. (A) Total number of bacteria (both *S. alvi* and *Gilliamella*) was determined by plating homogenized guts on BHIA and counting CFUs. Each dot represents a single bee gut and red bars represent the median value for each group, horizontal dotted line represents limit of detection (LOD = < 500). Wilcoxon rank sum test was done with *S. alvi* (Pollen -) as reference group, ns, nonsignificant; ****P < 0.001. (**B**) Bacterial cells (number of bacterial genome equivalents) per bee gut determined by qPCR using genus specific *Gilliamella* 16S rRNA gene primers. Each dot represents the number of cells in a single bee gut, red bars represent the median, horizontal black line represents qPCR limit of detection (LOD = < 7.5e+03). The presence of pollen in the diet is indicated by (P). Wilcoxon rank sum test was done with *Gilliamella* (Pollen -) as reference group, ns, nonsignificant; ****P < 0.001.

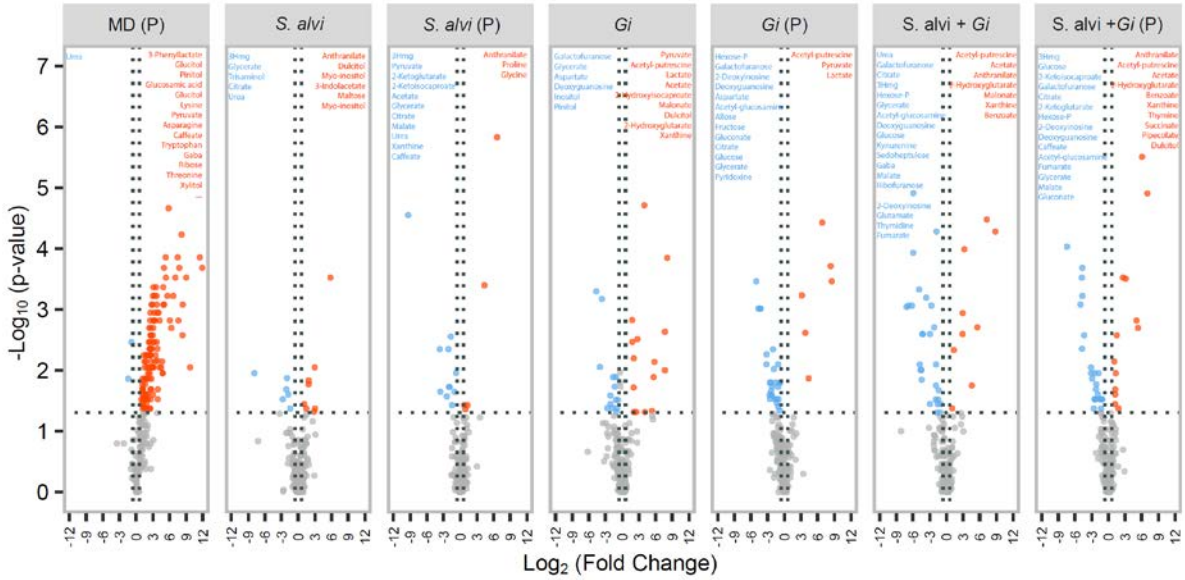

Figure S2. Volcano plots highlighting gut metabolite abundance changes between colonized and microbiota-depleted (MD) bees with and without pollen. Significantly differentially abundant metabolites between mono- and co-colonized *S. alvi* and *Gilliamella (Gi)* vs MD bees, as well as between MD (pollen+) and MD (pollen-) bees. Significantly depleted and produced metabolites are shown in blue and orange, respectively. Annotations are listed in order of significance for identified metabolites, with isomers and other duplications removed. The full set of significantly more abundant metabolites in the first panel can be found in the supporting scripts. Adjusted significance values were calculated using Wilcoxon rank sum test, and Benjamini-Hochberg correction, using the MD guts as a reference.

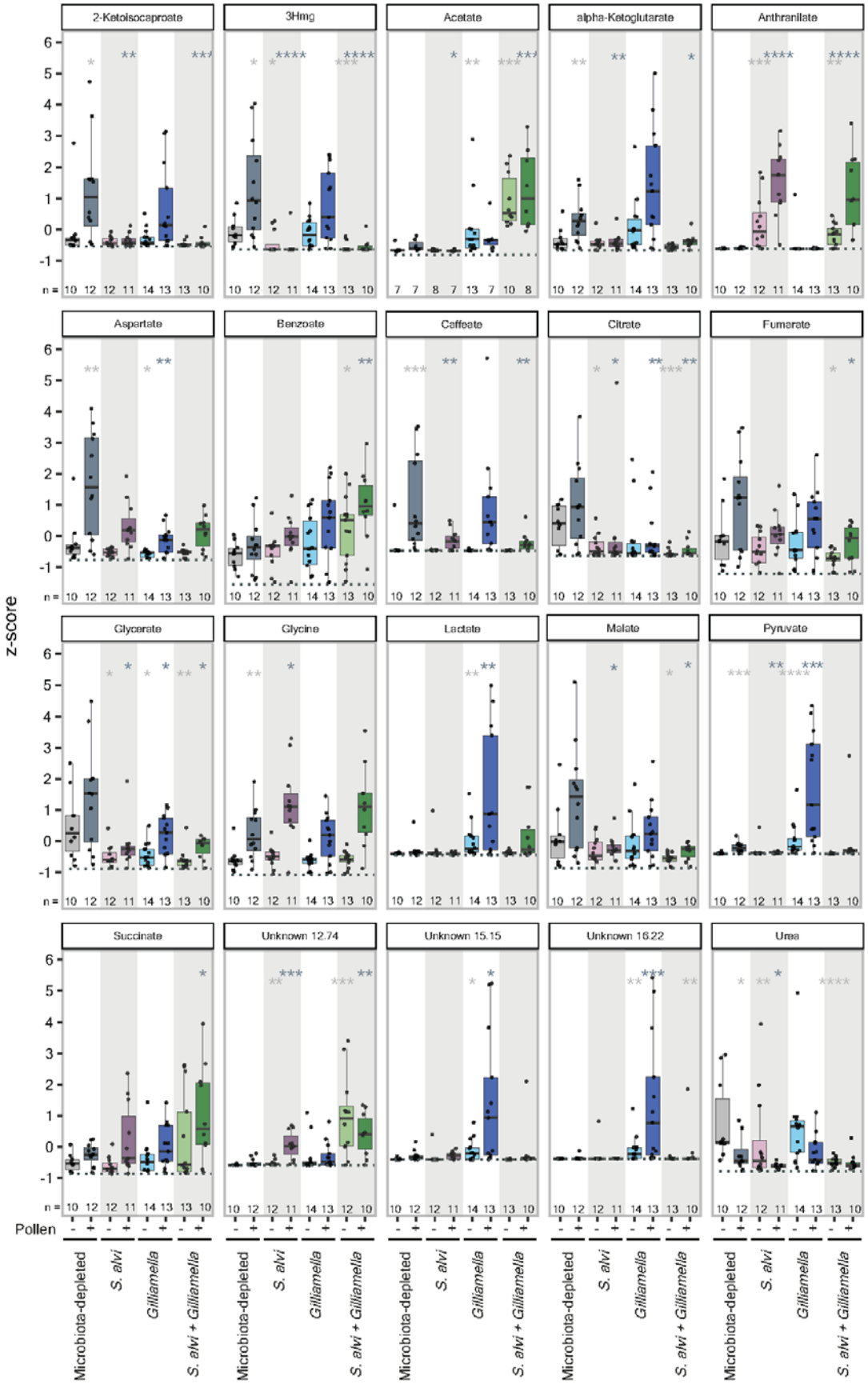
2-Ketoisocaproate
3Hmg
Acetate
alpha-Ketoglutarate
Anthranilate
Aspartate
Benzoate
Caffeate
Citrate
Fumarate
Glycerate
Glycine
Lactate
Malate
Pyruvate
Succinate
Unknown 12.74
Unknown 15.15
Unknown 16.22
Urea
z-score
n =
Pollen
Microbiota-depleted
S. alvi
Gilliamella
S. alvi + Gilliamella

589

Figure S3. Z-score normalized metabolite abundances of compounds significantly affected by *S. alvi* colonization. Box plots and individual data points display values across all 8 experimental conditions. Only metabolites in which a mixed linear model showed a significant effect of *S.* alvi colonization are plotted. Multiple types of metabolic interactions are shown. For example, metabolite depletion by *S. alvi* exclusively (2-Ketoisocaproate, 3Hmg, Caffeate, Urea) or by both species (Aspartate, Citrate, Glycerate), metabolite production by *S. alvi* exclusively (Anthranilate, Unknown 12.74), cross-feeding from *Gilliamella* to *S. alvi* (Pyruvate, Lactate), synergistic metabolite depletion (Fumarate, Malate) and production (Acetate, Benzoate). The light and dark gray asterisks show groups significantly different from MD (Pollen -) and MD (Pollen +) bees respectively, calculated using Wilcoxon rank sum test, * $P < 0.05$, ** < 0.01, *** < 0.001, **** < 0.0001. The dotted line represents the transformed limit of detection for each metabolite.

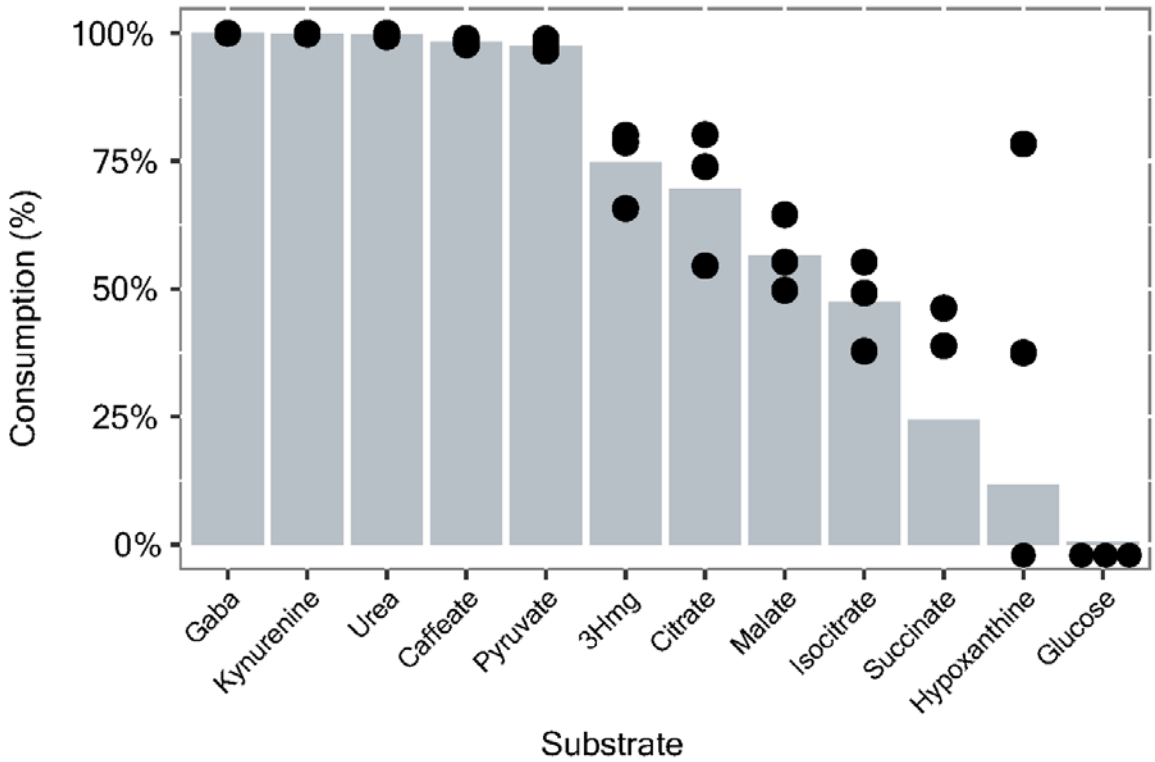

Figure S4. *In vitro* consumption of carbon substrates. The percentage of each carbon source consumed by the end of the *in vitro* growth experiment is shown for each tested carbon source. Data was taken from the condition in which all carbon sources were added to Bee9 media in equimolar amounts. Bars represent the average value from 3 biological replicates (black dots).

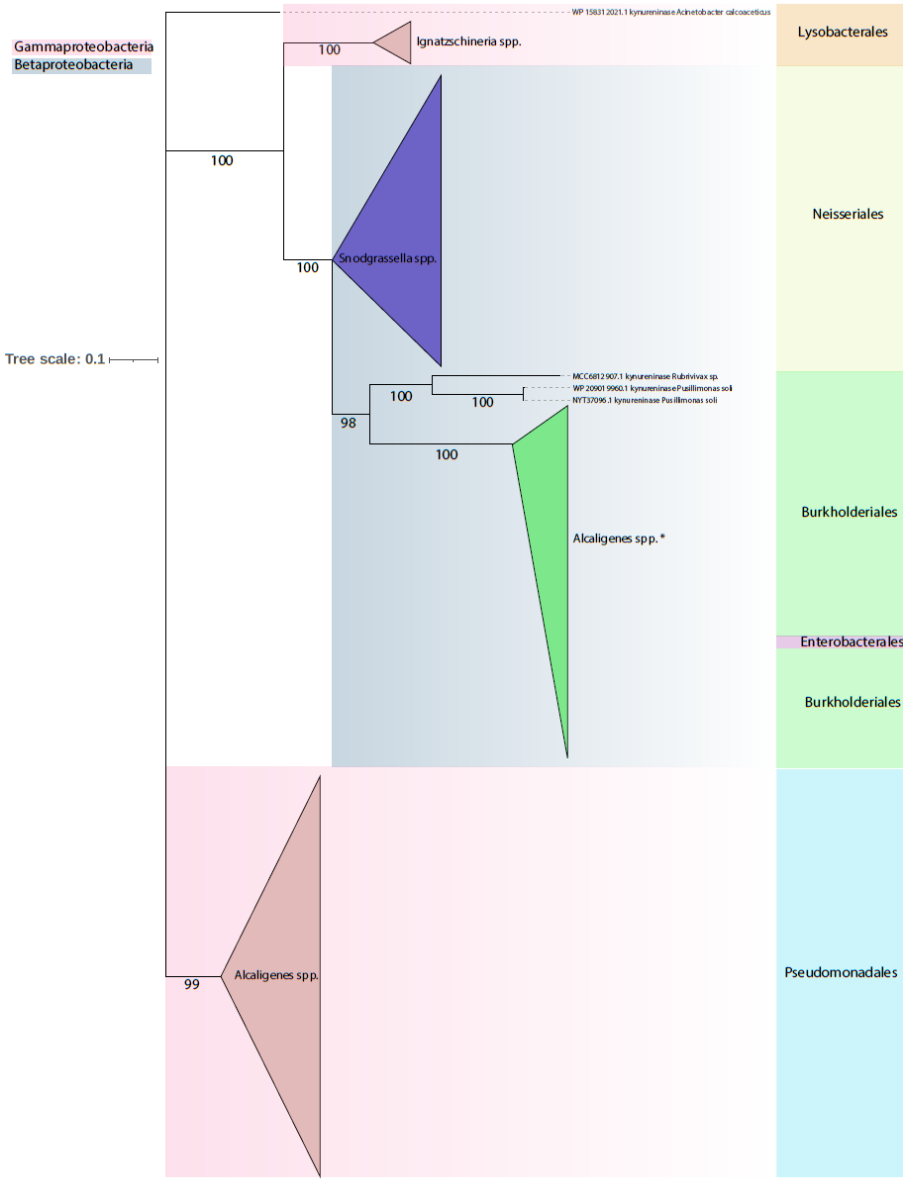

Figure S5. Phylogenetic tree of the kynureninase gene family found in *S. alvi*. The amino acid sequences of 227 homologs of the kynureninase gene identified in *S. alvi* wkb2 were retrieved from NCBI. The tree was inferred with Iqtree after aligning the sequences with MUSCLE (see methods). Tips are collapsed for clades that contain sequences of the same genus. Colored boxes on the right indicate the bacterial family. Bootstrap values are indicated before every node. Gammaproteobacteria are highlighted in pink and Betaproteobacteria in blue. Asterisk indicates a sequence (MBY6345856.1) from Providencia rettgeri, a Gammaproteobacterium, which clusters together with homologs of the kynureninase of Betaproteopbacteria.

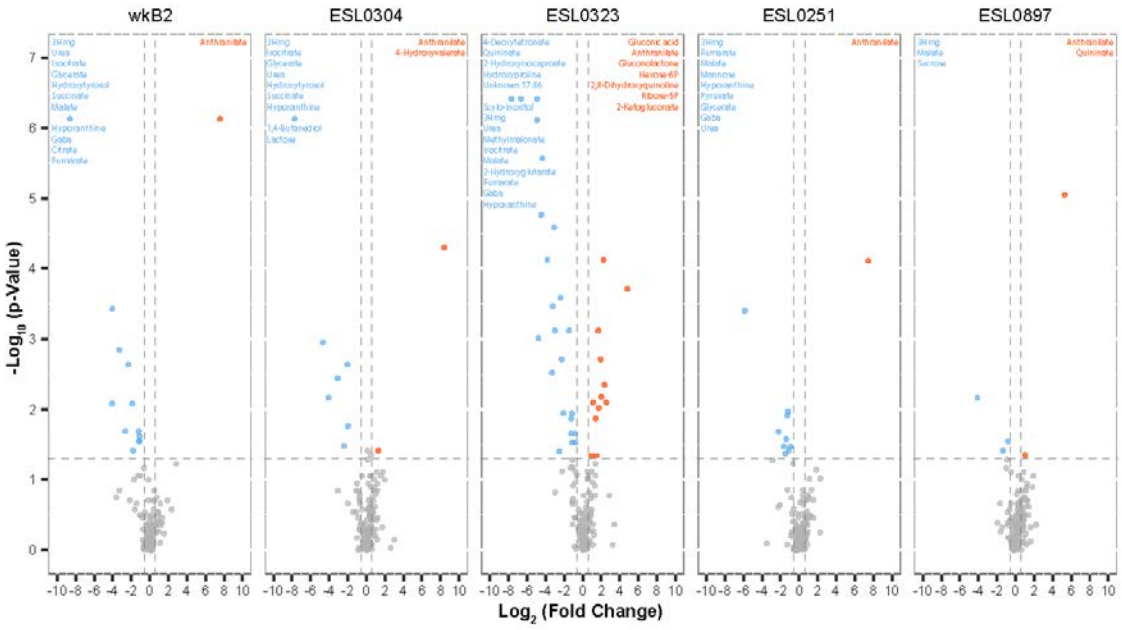

Figure S6. Gut metabolite changes in bees mono-colonized with divergent *S. alvi* strains relative to microbiota-depleted (MD) bees. Volcano plot of gut metabolites showing the similarities in metabolite changes from colonized vs MD bees across strains. Significantly depleted and produced metabolites are shown in blue and orange, respectively. Adjusted significance values were calculated using Wilcoxon rank sum test, and Benjamini-Hochberg correction, using the MD guts as a reference.

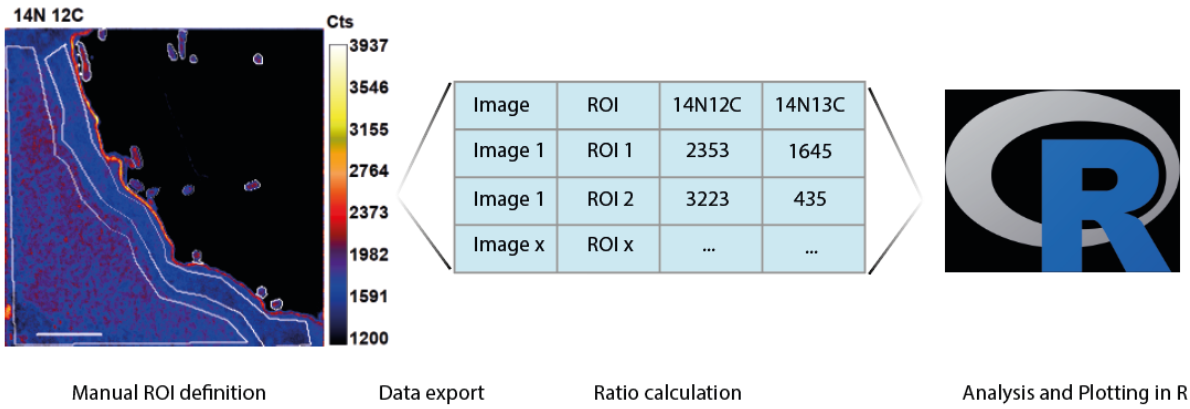

Figure S7. NanoSIMS image analysis workflow. For each image, 10 layers were acquired by bombarding the surface of the samples with Cs+ Ion beam (See methods). The image processing was performed using "L'image" software (Larry Nittler, Carnegie Institution of Washington). The 10 layers were aligned and stacked and 44 ms deadtime correction was applied. Regions of interests (ROI) were manually drawn around bacterial cells, gut epithelium layer, and bulk host cells, using a minimum threshold specified and values were extracted and reported in **Dataset S1**. At% enrichment was calculated in R using the data.table package. At% enrichment formula: $13C\ At\% = {}^{14\mathrm{N}\ 13\mathrm{C}}/_{(14\mathrm{N}\ 13\mathrm{C}\ +\ 14\mathrm{N}\ 12\mathrm{C})} \times 100.$

Table S1. Bacterial strains used in this study. [12,50,51]

Bacterial strain	# 16S rRNA copies	Culturing condition	Strain source	Place of origin
Gilliamella apicola wkB1^{T}	4	BHIA, 35°C, microaerophilic	(Kwong & Moran, 2013)	New Haven, USA
Gilliamella apis ESL0169	4	BHIA, 35°C, microaerophilic	(Kešnerová et al., 2017)	Lausanne, Switzerland
Gilliamella sp. ESL0182	4	BHIA, 35°C, microaerophilic	(Ellegaard & Engel, 2018)	Lausanne, Switzerland
Gilliamella apis ESL0297	4	BHIA, 35°C, microaerophilic	This study	Lausanne, Switzerland
Snodgrassella alvi wkB2^{T}	4	TSA, 35°C, microaerophilic	(Kwong & Moran, 2013)	New Haven, USA
Snodgrassella alvi ESL0304	4	TSA, 35°C, microaerophilic	This study	Lausanne, Switzerland
Snodgrassella alvi ESL0323	4	TSA, 35°C, microaerophilic	This study	Lausanne, Switzerland
Snodgrassella alvi ESL0251	4	TSA, 35°C, microaerophilic	This study	Lausanne, Switzerland
Snodgrassella alvi ESL0897	4	TSA, 35°C, microaerophilic	This study	Lausanne, Switzerland

Table S2. *S. alvi* & *Gilliamella* colonization summary counts. Total bee numbers per experiment, survival rate, and number of bees used for CFU plating, qPCR and metabolomics analysis are shown.

	Replicate	1	2	3	4	5	Total
Bees	MD	34	24	24	24	0	106
	MD (P)	30	23	23	25	0	101
	Sn	31	24	20	0	20	95
	Sn (P)	34	23	20	0	19	96
	Sn+Gi	32	22	24	0	16	94
	Sn+Gi (P)	29	24	20	0	22	95
	Gi	0	0	0	26	25	51
	Gi (P)	0	0	0	25	25	50
Survival (%)	MD	100%	100%	100%	96%	N/A	99%
	MD (P)	100%	100%	100%	100%	N/A	100%
	Sn	94%	100%	100%	N/A	100%	98%
	Sn (P)	100%	100%	95%	N/A	100%	99%
	Sn+Gi	97%	95%	100%	N/A	100%	98%
	Sn+Gi (P)	97%	92%	95%	N/A	100%	96%
	Gi	N/A	N/A	N/A	100%	100%	100%
	Gi (P)	N/A	N/A	N/A	96%	100%	98%
CFU	MD	10	10	10	10	N/A	40
	MD (P)	10	10	10	10	N/A	40
	Sn	10	10	10	N/A	6	36
	Sn (P)	10	10	10	N/A	6	36
	Sn+Gi	10	10	10	N/A	6	36
	Sn+Gi (P)	10	10	10	N/A	6	36
	Gi	N/A	N/A	N/A	10	18	28
	Gi (P)	N/A	N/A	N/A	10	18	28
qPCR	MD	4	3	4	6	N/A	25
	MD (P)	4	3	4	5	N/A	24
	Sn	4	9	6	N/A	6	33
	Sn (P)	4	9	8	N/A	6	35
	Sn/Gi	10	10	11	N/A	6	46
	Sn/Gi (P)	10	10	10	N/A	6	46
	Gi	N/A	N/A	N/A	10	14	40
	Gi (P)	N/A	N/A	N/A	9	21	47
Metabolomics	MD	2	1	2	5	N/A	10
	MD (P)	2	1	4	5	N/A	12
	Sn	1	1	2	N/A	6	10
	Sn (P)	1	1	3	N/A	6	11
	Sn+Gi	3	1	5	N/A	6	15
	Sn+Gi (P)	1	1	4	N/A	5	11
	Gi	N/A	N/A	N/A	5	9	14
	Gi (P)	N/A	N/A	N/A	6	7	13

Table S3. Summary of the number of bees sampled per replicate and treatment for the mono-colonization experiment with divergent *Snodgrassella* strains. Total number of bees per experiment, survival rate, and number of bees used for CFU plating and metabolomics analysis are shown.

	Replicate	1	2	Total
Bees	MD	14	15	29
	wkB2	14	14	28
	251	16	15	31
	304	14	15	29
	323	14	15	29
	892	14	15	29
	897	15	14	29
Survival (%)	MD	93%	100%	96%
	wkB2	100%	100%	100%
	251	88%	100%	94%
	304	100%	80%	90%
	323	100%	100%	100%
	892	86%	100%	93%
	897	80%	79%	79%
CFU	MD	12	12	24
	wkB2	12	12	24
	251	11	12	23
	304	12	9	21
	323	12	12	24
	892	12	12	24
	897	12	9	21
Metabolomics	MD	6	6	12
	wkB2	6	6	12
	251	8	9	17
	304	6	6	12
	323	7	6	13
	892	6	6	12
	897	6	6	12

Data Availability

Raw data and scripts used to process data and generate figures are available on github at the following link: https://github.com/Yelchazli/Foraging-on-host-synthesized-metabolites-enables-S.-alvi-to-colonize-the-honey-bee-gut/blob/main/README.md.

Acknowledgments

We would like to thank Silvia Morian-Gutierrez, and Gonçalo Santos-Matos for providing helpful comments on the manuscript. This work was funded by the University of Lausanne, an ERC Starting Grant (MicroBeeOme), the NCCR Microbiomes, a National Centre of Competence in Research, funded by the Swiss National Science Foundation (grant no. 180575) and a Swiss National Science Foundation project grant (grant no. 179487) to P.E.

Author Contributions

A.Q., Y.E. and P.E. conceived the project and designed the experiments. A.Q, and Y.E. performed the experiments. A.Q. analyzed the GC-MS results, while Y.E. analyzed the qPCR and NanoSIMS results. N.N. assisted with bee experiments, metabolite, and DNA extractions. A.M.N. performed preliminary in vitro growth experiments. J.D. performed the tissue sectioning and TEM imaging supervised by C.G. S.E. performed the NanoSIMS imaging and instructed on the data analysis, supervised by A.M., who also advised on the design of the NanoSIMS experiment. A.Q., Y.E. and P.E. wrote the manuscript, with contributions from S.E. and A.M. All authors reviewed the manuscript and provided feedback.

References

1 Tremaroli, V. & Bäckhed, F. Functional interactions between the gut microbiota and host metabolism. *Nature* **489**, 242-249, doi:10.1038/nature11552 (2012).

2 Kwong, W. K. & Moran, N. A. Gut microbial communities of social bees. *Nature Reviews Microbiology* **14**, 374-384, doi:10.1038/nrmicro.2016.43 (2016).

3 Bonilla-Rosso, G. & Engel, P. Functional roles and metabolic niches in the honey bee gut microbiota. *Current Opinion in Microbiology* **43**, 69-76, doi:10.1016/j.mib.2017.12.009 (2018).

4 Kwong, W. K. *et al.* Dynamic microbiome evolution in social bees. *Science Advances* **3**, e1600513, doi:doi:10.1126/sciadv.1600513 (2017).

5 Li, Y., Leonard, S. P., Powell, J. E. & Moran, N. A. Species divergence in gut-restricted bacteria of social bees. *Proceedings of the National Academy of Sciences* **119**, e2115013119, doi:doi:10.1073/pnas.2115013119 (2022).

6 Wu, J. *et al.* Honey bee genetics shape the strain-level structure of gut microbiota in social transmission. *Microbiome* **9**, 225, doi:10.1186/s40168-021-01174-y (2021).

7 Engel, P. *et al.* Standard methods for research on Apis mellifera gut symbionts. *Journal of Apicultural Research* **52**, 1-24, doi:10.3896/ibra.1.52.4.07 (2013).

8 Ricigliano, V. A. & Anderson, K. E. Probing the Honey Bee Diet-Microbiota-Host Axis Using Pollen Restriction and Organic Acid Feeding. *Insects* **11**, 291 (2020).

9 Zheng, H., Steele, M. I., Leonard, S. P., Motta, E. V. S. & Moran, N. A. Honey bees as models for gut microbiota research. *Lab Animal* **47**, 317-325, doi:10.1038/s41684-018-0173-x (2018).

10 Kwong, W. K., Engel, P., Koch, H. & Moran, N. A. Genomics and host specialization of honey bee and bumble bee gut symbionts. *Proceedings of the National Academy of Sciences* **111**, 11509-11514, doi:doi:10.1073/pnas.1405838111 (2014).

11 Martinson, V. G., Moy, J. & Moran, N. A. Establishment of characteristic gut bacteria during development of the honeybee worker. *Appl Environ Microbiol* **78**, 2830-2840, doi:10.1128/aem.07810-11 (2012).

12 Kešnerová, L. *et al.* Disentangling metabolic functions of bacteria in the honey bee gut. *PLOS Biology* **15**, e2003467, doi:10.1371/journal.pbio.2003467 (2017).

13 Schwartzman, J. A. *et al.* The chemistry of negotiation: Rhythmic, glycan-driven acidification in a symbiotic conversation. *Proceedings of the National Academy of Sciences* **112**, 566-571, doi:doi:10.1073/pnas.1418580112 (2015).

14 Desai, M. S. *et al.* A Dietary Fiber-Deprived Gut Microbiota Degrades the Colonic Mucus Barrier and Enhances Pathogen Susceptibility. *Cell* **167**, 1339-1353.e1321, doi:https://doi.org/10.1016/j.cell.2016.10.043 (2016).

15 Sonnenburg, J. L. *et al.* Glycan Foraging in Vivo by an Intestine-Adapted Bacterial Symbiont. *Science* **307**, 1955-1959, doi:doi:10.1126/science.1109051 (2005).

16 Berry, D. *et al.* Host-compound foraging by intestinal microbiota revealed by single-cell stable isotope probing. *Proceedings of the National Academy of Sciences* **110**, 4720-4725, doi:doi:10.1073/pnas.1219247110 (2013).

17 Sicard, J.-F., Le Bihan, G., Vogeleer, P., Jacques, M. & Harel, J. Interactions of Intestinal Bacteria with Components of the Intestinal Mucus. *Frontiers in Cellular and Infection Microbiology* **7**, doi:10.3389/fcimb.2017.00387 (2017).

18 Martens, E. C., Chiang, H. C. & Gordon, J. I. Mucosal Glycan Foraging Enhances Fitness and Transmission of a Saccharolytic Human Gut Bacterial Symbiont. *Cell Host & Microbe* **4**, 447-457, doi:10.1016/j.chom.2008.09.007 (2008).

19 Miyashiro, T. *et al.* The N-acetyl-d-glucosamine repressor NagC of Vibrio fischeri facilitates colonization of Euprymna scolopes. *Molecular Microbiology* **82**, 894-903, doi:https://doi.org/10.1111/j.1365-2958.2011.07858.x (2011).

20 Wier, A. M. *et al.* Transcriptional patterns in both host and bacterium underlie a daily rhythm of anatomical and metabolic change in a beneficial symbiosis. *Proceedings of the National Academy of Sciences* **107**, 2259-2264, doi:doi:10.1073/pnas.0909712107 (2010).

21 Gillis, C. C. *et al.* Dysbiosis-Associated Change in Host Metabolism Generates Lactate to Support Salmonella Growth. *Cell Host & Microbe* **23**, 54-64.e56, doi:https://doi.org/10.1016/j.chom.2017.11.006 (2018).

22 Rosenberg, G. *et al.* Host succinate is an activation signal for Salmonella virulence during intracellular infection. *Science* **371**, 400-405, doi:doi:10.1126/science.aba8026 (2021).

23 Nguyen, B. D. *et al.* Import of Aspartate and Malate by DcuABC Drives H2/Fumarate Respiration to Promote Initial Salmonella Gut-Lumen Colonization in Mice. *Cell Host & Microbe* **27**, 922-936.e926, doi:10.1016/j.chom.2020.04.013 (2020).

24 Zeng, X. *et al.* Gut bacterial nutrient preferences quantified in vivo. *Cell* **185**, 3441-3456.e3419, doi:10.1016/j.cell.2022.07.020 (2022).

25 Zheng, H., Powell, J. E., Steele, M. I., Dietrich, C. & Moran, N. A. Honeybee gut microbiota promotes host weight gain via bacterial metabolism and hormonal signaling. *Proceedings of the National Academy of Sciences* **114**, 4775-4780, doi:doi:10.1073/pnas.1701819114 (2017).

26 Brochet, S. *et al.* Niche partitioning facilitates coexistence of closely related honey bee gut bacteria. *eLife* **10**, doi:10.7554/elife.68583 (2021).

27 Powell, J. E., Leonard, S. P., Kwong, W. K., Engel, P. & Moran, N. A. Genome-wide screen identifies host colonization determinants in a bacterial gut symbiont. *Proceedings of the National Academy of Sciences* **113**, 13887-13892, doi:doi:10.1073/pnas.1610856113 (2016).

28 Kwong, W. K., Zheng, H. & Moran, N. A. Convergent evolution of a modified, acetate-driven TCA cycle in bacteria. *Nature Microbiology* **2**, 17067, doi:10.1038/nmicrobiol.2017.67 (2017).

29 Sharp, C. & Foster, K. R. Host control and the evolution of cooperation in host microbiomes. *Nature Communications* **13**, 3567, doi:10.1038/s41467-022-30971-8 (2022).

30 Steele, M. I., Motta, E. V. S., Gattu, T., Martinez, D. & Moran, N. A. The Gut Microbiota Protects Bees from Invasion by a Bacterial Pathogen. *Microbiology Spectrum* **9**, e00394-00321, doi:doi:10.1128/Spectrum.00394-21 (2021).

31 Cerstiaens, A. *et al.* Neurotoxic and neurobehavioral effects of kynurenines in adult insects. *Biochemical and Biophysical Research Communications* **312**, 1171-1177, doi:https://doi.org/10.1016/j.bbrc.2003.11.051 (2003).

32 Marszalek-Grabska, M. *et al.* Kynurenine emerges from the shadows – Current knowledge on its fate and function. *Pharmacology & Therapeutics* **225**, 107845, doi:https://doi.org/10.1016/j.pharmthera.2021.107845 (2021).

33 Schwarcz, R. & Stone, T. W. The kynurenine pathway and the brain: Challenges, controversies and promises. *Neuropharmacology* **112**, 237-247, doi:https://doi.org/10.1016/j.neuropharm.2016.08.003 (2017).

34 Scheiner, R., Baumann, A. & Blenau, W. Aminergic control and modulation of honeybee behaviour. *Curr Neuropharmacol* **4**, 259-276, doi:10.2174/157015906778520791 (2006).

35 Zhang, Z. *et al.* Honeybee gut Lactobacillus modulates host learning and memory behaviors via regulating tryptophan metabolism. *Nature Communications* **13**, 2037, doi:10.1038/s41467-022-29760-0 (2022).

36 Hu, Y. *et al.* Herbivorous turtle ants obtain essential nutrients from a conserved nitrogen-recycling gut microbiome. *Nature Communications* **9**, 964, doi:10.1038/s41467-018-03357-y (2018).

37 Kešnerová, L. *et al.* Gut microbiota structure differs between honeybees in winter and summer. *The ISME Journal* **14**, 801-814, doi:10.1038/s41396-019-0568-8 (2020).

38 Nocelli, R. C., Cintra-Socolowski, P., Roat, T. C., Silva-Zacarin, E. C. M. & Malaspina, O.

39 Yagi, S. & Ogawa, H. Effect of Tryptophan Metabolites on Fluorescent Granules in the Malpighian Tubules of Eye Color Mutants of Drosophila melanogaster. *Zoological Science* **13**, 97-104, 108 (1996).

40 Emery, O., Schmidt, K. & Engel, P. Immune system stimulation by the gut symbiont Frischella perrara in the honey bee (Apis mellifera). *Molecular Ecology* **26**, 2576-2590, doi:https://doi.org/10.1111/mec.14058 (2017).

41 den Besten, G. *et al.* The Short-Chain Fatty Acid Uptake Fluxes by Mice on a Guar Gum Supplemented Diet Associate with Amelioration of Major Biomarkers of the Metabolic Syndrome. *PLOS ONE* **9**, e107392, doi:10.1371/journal.pone.0107392 (2014).

42 Fiehn, O. *et al.* Quality control for plant metabolomics: reporting MSI-compliant studies. *The Plant Journal* **53**, 691-704, doi:10.1111/j.1365-313x.2007.03387.x (2008).

43 Wanichthanarak, K., Jeamsripong, S., Pornputtapong, N. & Khoomrung, S. Accounting for biological variation with linear mixed-effects modelling improves the quality of clinical metabolomics data. *Computational and Structural Biotechnology Journal* **17**, 611-618, doi:https://doi.org/10.1016/j.csbj.2019.04.009 (2019).

44 Nargund, S., Misra, A., Zhang, X., Coleman, G. D. & Sriram, G. Flux and reflux: metabolite reflux in plant suspension cells and its implications for isotope-assisted metabolic flux analysis. *Molecular BioSystems* **10**, 1496-1508, doi:10.1039/C3MB70348G (2014).

45 Rosenblatt, J., Chinkes, D., Wolfe, M. & Wolfe, R. R. Stable isotope tracer analysis by GC-MS, including quantification of isotopomer effects. *American Journal of Physiology-Endocrinology and Metabolism* **263**, E584-E596, doi:10.1152/ajpendo.1992.263.3.E584 (1992).

46 Kremer, J. R., Mastronarde, D. N. & McIntosh, J. R. Computer Visualization of Three-Dimensional Image Data Using IMOD. *Journal of Structural Biology* **116**, 71-76, doi:https://doi.org/10.1006/jsbi.1996.0013 (1996).

47 Hoppe, P., Cohen, S. & Meibom, A. NanoSIMS: Technical Aspects and Applications in Cosmochemistry and Biological Geochemistry. *Geostandards and Geoanalytical Research* **37**, 111-154, doi:https://doi.org/10.1111/j.1751-908X.2013.00239.x (2013).

48 Edgar, R. C. MUSCLE: multiple sequence alignment with high accuracy and high throughput. *Nucleic Acids Res* **32**, 1792-1797, doi:10.1093/nar/gkh340 (2004).

49 Nguyen, L. T., Schmidt, H. A., von Haeseler, A. & Minh, B. Q. IQ-TREE: a fast and effective stochastic algorithm for estimating maximum-likelihood phylogenies. *Mol Biol Evol* **32**, 268-274, doi:10.1093/molbev/msu300 (2015).

50 Kwong, W. K. & Moran, N. A. Cultivation and characterization of the gut symbionts of honey bees and bumble bees: description of Snodgrassella alvi gen. nov., sp. nov., a member of the family Neisseriaceae of the. *International Journal of Systematic and Evolutionary Microbiology* **63**, 2008-2018, doi:10.1099/ijs.0.044875-0 (2013).

51 Ellegaard, K. M. & Engel, P. New Reference Genome Sequences for 17 Bacterial Strains of the Honey Bee Gut Microbiota. *Microbiol Resour Announc* **7**, doi:10.1128/mra.00834-18 (2018).